STRESS DISTRIBUTION AND DEFORMATION IN A TWISTED BLADE UNDER COMBINED TENSION AND TORSION

LAWRENCE MILES HOGAN

STRESS DISTRIBUTION AND DEFORMATION IN A TWISTED BLADE UNDER COMBINED TENSION AND TORSION

by

Lawrence Miles Hogan
Lieutenant Commander, United States Navy
B.S., United States Naval Academy, 1957

Submitted in partial fulfillment
for the degree of

MASTER OF SCIENCE IN AERONAUTICAL ENGINEERING

from the

UNITED STATES NAVAL POSTGRADUATE SCHOOL

May 1966

ABSTRACT

A theoretical and experimental investigation of the stress distribution and deformation of twisted blades under combined tension and torsion was conducted by LCDR Lawrence M. Hogan, USN, at the Aeronautical Engineering Department of the U. S. Naval Postgraduate School, Monterey, California. Theoretical expressions were developed to relate the deformation of a twisted "blade" of rectangular cross section and constant rate of twist to an applied load and moment. These expressions were found to be linear for the rates of twist investigated and depended only on the blade material and geometry. The theoretical strain distribution was found to be essentially parabolic across the chord, with the shape determined by the initial twist rate and the angular deformation.

The experimental investigation was conducted with three specimens of constant cross sectional aspect ratio but different rates of twist. Correlation with theory was found to be excellent for the chordwise distribution of strain and generally good for the linear relationships linking the deformation with the applied loads. Recommendations were made for areas of further investigation.

TABLE OF CONTENTS

LIST OF TABLES

LIST OF ILLUSTRATIONS

TABLE OF SYMBOLS

a	Maximum radius of helical blade
e_t	Strain along the tangent to the helix
e_o	Strain at the longitudinal axis of the blade
E	Young's modulus
f	Multiplying factor to convert torsion theory for a rectangular bar to that for a twisted bar
G	Shear modulus
h	Maximum width of cross section of the helical blade
K	Non-dimensional initial twist rate, $a\frac{d\theta}{dz}$
L	Length of twisted blade
P	Applied tensile load
P^*	Non-dimensional applied tensile load, $\frac{P}{2ahE}$
r	Radius of helical blade
R	Radius of cutter bit used to machine specimens
t	Thickness of helical blade in the direction normal to the middle surface
T	Applied moment
T^*	Non-dimensional applied moment, $\frac{T}{2a^2hE}$
u	Longitudinal displacement
z	Direction of or distance along the longitudinal axis
α	Constants in the expressions for P^* and T^*
β	Constants in the expressions for e_o and χ
θ	Initial angle of twist
μ	Poisson's ratio
ξ	Non-dimensional blade radius, r/a

σ_t Membrane stress in the direction of the tangent to the helix

γ Non-dimensional cutter radius, $\frac{R}{h}$

ϕ Helix angle

χ Non-dimensional angular deformation, a $\frac{d\psi}{dz}$

ψ Angular deformation

$( )'$ Refers to differentiation with respect to z, $\frac{d( )}{dz}$

1. Introduction.

An analysis of the stress distribution and the distortion of twisted blades subjected to combined tensile and torsional loads has several fundamental engineering applications. Propeller and turbine blades are two examples of the special case in which the blade is under tension but essentially free of torsion. High rotational velocities place these blades in tension due to centrifugal force while only an insignificant amount of torsion results from the aerodynamic loads on the blade. The need to predict the resultant stress distribution and accompanying distortion of these blades is evident.

This paper is an attempt to evaluate the applicability of a simple theoretical approach to this problem. Specifically, the analysis involves a twisted "blade" of constant rectangular cross section and constant rate of twist, subjected to known applied torsional and tensile loads. The predicted results for three different rates of twist are compared with experimental results obtained from three test specimens.

The strain at any chordwise station is determined from an analysis of the geometry of the twisted blade. All deformations are restricted to the elastic region. The central chordline of the blade passes perpendicularly through the longitudinal axis. A key assumption is that this chordline, originally straight, remains straight in the deformed state. Thus the displacement of a chordline a small distance from a reference chordline is expressed as a linear displacement in the longitudinal direction and a rotation about the blade axis. The strain at any chordwise station is established as being dependent on initial rate

of twist, on the longitudinal strain at the centerline, and on the angular deformation.

The basis for the theoretical analysis can best be described as modified membrane theory. Expressions are obtained for an applied tensile force and for an applied moment in terms of membrane stress and the associated geometry of the blade. The stresses are then expressed in terms of the previously determined strain relationships by means of Hooke's Law. This allows the applied force and moment to be expressed in a form linearly dependent on the longitudinal strain at the centerline, e_o, and on the non-dimensional angular deformation, χ. These solutions are modified by the torsional relationships for a twisted prismatical bar of rectangular cross section. The resultant linear expressions are then inverted to solve for e_o and χ in terms of the applied tensile and torsional loads.

Test data was obtained to compare the actual relationships with those predicted by theory for two special cases of applied load and moment: 1) An applied tensile load with zero applied moment and 2) an applied moment with zero applied tensile load.

2. Analysis.

A diagram of the model to be analyzed is shown in Fig. 1. The model is considered to be an axisymmetric helical blade machined from a circular rod. The angle of twist, represented by θ in view (a), varies uniformly over the length, L, giving $\frac{d\theta}{dz}$ = constant. The edge of the blade describes a helix, the projection of which is a sine wave as is evident in view (b). Any cross section of the blade normal to the z-axis is essentially a rectangle of length 2a and width, h.

The helix angle, ϕ, describes the angular difference between the tangent to the helix at any radius, r, and a line parallel to the z-axis, as shown in view (c). Thus ϕ varies linearly with r from zero at r = 0 to ϕ_{max} at r = a.

As a first approximation in the analysis, the blade thickness is assumed very small so that it approaches a pure membrane. The blade is therefore considered to have zero bending stiffness and the applied load must be taken by tensile stresses in the center surface of the blade. An inspection of the applied load, P and T, shows the stress in the radial direction to be zero. Therefore, the significant stress for this analysis is that represented by σ_t, the stress directed along the tangent to the helix. Considering then the element of cross section surface on which σ_t acts, tdr, the elemental membrane tensile force is represented by $\sigma_t t dr$, view (c). The component of the tensile force in the z direction, $\sigma_t t dr \cos \phi$, integrated over the chord must be equal to any applied tensile load, P. The component of the tensile force perpendicular to the z-axis, $\sigma_t t dr \sin \phi$, introduces a moment about the

centerline since it acts at a distance r from the axis. Thus the integrated moment over the chord must be equated to the applied moment, T. These relationships are expressed in eqns. (1) and (2).

$$P = \int_{-a}^{a} \sigma_t t dr \cos \phi \tag{1}$$

$$T = \int_{-a}^{a} \sigma_t t r dr \sin \phi \tag{2}$$

The assumption of a rectangular cross section is not exact in actuality due to the machining process. The blades herein analyzed were machined from round stock. The stock was mounted in a manner so as to pass spirally by a cutting bit, as illustrated in Fig. 2. If this cutting bit were of infinitesimally small radius, it would act only at a particular z-station and an exact rectangle would be formed in the cross section normal to the z-axis (neglecting the arc on the ends). The finite radius of this bit caused it to machine on adjacent z-stations as well, introducing a variation in the thickness across the cross section. Thus the thickness t can be found from Fig. 2 to be

$$t = h \cos \phi - 2R(1 - \cos \phi) \tag{3}$$

where R is the radius of the cutting bit.

Rearranging and defining the non-dimensional cutter bit radius, γ, as R/h gives

$$t = h\left[\cos \phi - 2 \gamma (1 - \cos \phi)\right] \tag{4}$$

Fig. 3 shows an elemental length of blade, dz. Line OP is the helical path at radius r over the elemental length. The circumferential displacement over the length dz is seen to be $rd\theta$. Thus the helix angle, ϕ, is defined by

$$\phi = \tan^{-1} \frac{rd\theta}{dz} \tag{5}$$

The non-dimensional rate of twist, K, and the non-dimensional radius, ξ, are defined as

$$K = a \frac{d\theta}{dz} \tag{6}$$

$$\xi = \frac{r}{a} \tag{7}$$

Thus eqn. (5) becomes

$$\phi = \tan^{-1} K\xi \tag{8}$$

giving

$$\phi_{max} = \tan^{-1} K \tag{9}$$

$$\sin \phi = \frac{K\xi}{\sqrt{1 + K^2\xi^2}} \tag{10}$$

$$\cos \phi = \frac{1}{\sqrt{1 + K^2\xi^2}} \tag{11}$$

$$1 - \cos\phi = 1 - \frac{1}{\sqrt{1+\kappa^2\xi^2}} = \frac{\sqrt{1+\kappa^2\xi^2} - 1}{\sqrt{1+\kappa^2\xi^2}} \qquad (12)$$

The radical in the numerator of eqn. (12) can be expanded by the binomial theorem to give

$$\sqrt{1+\kappa^2\xi^2} = 1 + \tfrac{1}{2}\kappa^2\xi^2 - \tfrac{1}{8}\kappa^4\xi^4 + \cdots \qquad (13)$$

Dropping higher order terms there is

$$1 - \cos\phi = \frac{\frac{1}{2}\kappa^2\xi^2}{\sqrt{1+\kappa^2\xi^2}} \qquad (14)$$

Thus eqn. (4) becomes

$$t = h\,\frac{1 - r\kappa^2\xi^2}{\sqrt{1+\kappa^2\xi^2}} \qquad (15)$$

Substituting these expressions back into eqns. (1) and (2) and changing the variable of integration from dr to $d\xi$, produces

$$P = 2ah\int_0^1 \sigma_t\,\frac{1 - r\kappa^2\xi^2}{1+\kappa^2\xi^2}\,d\xi \qquad (16)$$

$$T = 2a^2h\int_0^1 \sigma_t\,\frac{\kappa\xi^2(1 - r\kappa^2\xi^2)}{1+\kappa^2\xi^2}\,d\xi \qquad (17)$$

Now an expression for σ_t in terms of deformations will be derived. Referring once again to Fig. 3, an important simplifying assumption is made which claims that the radius SP, originally a straight line normal to the z-axis, remains a straight line normal to the z-axis in the deformed state, S'P'.

The unstrained length of an element along the tangent is

$$OP = \frac{dz}{\cos \phi} = dz\sqrt{1 + \kappa^2 \xi^2} \qquad (19)$$

The strained condition is defined by a change in length parallel to the z-axis, du, and an angular change, $d\psi$. The length along the tangent to the helix in the strained condition, OP', is found as follows:

$$OP' = \sqrt{(dz + du)^2 + [r(d\theta + d\psi)]^2}$$

$$OP' = dz\sqrt{(1 + u')^2 + [r(\theta' + \psi')]^2}$$

$$OP' = dz\sqrt{(1 + u')^2 + \kappa^2 \xi^2 (1 + \psi'/\theta')^2}$$

Replacing u' and ψ'/θ' by the non-dimensional values e_o and χ/K, respectively, and expanding gives

$$OP' = dz\sqrt{1 + 2e_o + e_o^2 + \kappa^2 \xi^2 (1 + 2\chi/\kappa + \chi^2/\kappa^2)}$$

$$OP' = dz\sqrt{(1 + \kappa^2 \xi^2) + [e_o(2 + e_o) + \chi\kappa\xi^2(2 + \chi/\kappa)]}$$

$$OP' = dz\sqrt{1 + \kappa^2 \xi^2}\sqrt{1 + \frac{e_o(2 + e_o) + \chi\kappa\xi^2(2 + \chi/\kappa)}{1 + \kappa^2 \xi^2}} \qquad (20)$$

The strain along the tangent is now expressed by e_t.

$$e_t = \frac{OP' - OP}{OP}$$

$$e_t = \sqrt{1 + \frac{e_o(2+e_o) + \chi K \xi^2 (2 + \chi/K)}{1 + K^2 \xi^2}} - 1 \qquad (21)$$

The radical may be expressed as the binomial expansion of $(1 + F)^{1/2}$ and substituted as follows:

$$e_t = \left(1 + \tfrac{1}{2} F - \tfrac{1}{8} F^2 + \cdots\right) - 1$$

$$e_t = \tfrac{1}{2} F - \tfrac{1}{8} F^2 + \cdots \qquad (22)$$

Eqn. (22) is therefore the strain along the tangent to the helix at any radius, ξ . An order of magnitude analysis of the F term is now desired for simplifying purposes. e_o will be very small compared to unity, as will be χ/K if "large" initial twist rates are considered; i.e., if the ratio of angular deformation to initial twist is small. Neglecting these terms, F in eqn. (22) becomes

$$F_1 = 2 \frac{e_o + \chi K \xi^2}{1 + K^2 \xi^2} \qquad (23)$$

The denominator of F_1 is of the order of magnitude unity while the numerator is of much smaller order. It is therefore possible to neglect powers of F_1 and the expression for e_t becomes

$$e_t = \tfrac{1}{2} F_1 = \frac{e_o + \chi K \xi^2}{1 + K^2 \xi^2} \qquad (24)$$

Eqn. (24) is the simplified expression for the strain along the tangent at radius ξ . It can be rearranged to produce a linear relationship

between $e_t\ (1 + K^2 \xi^2)$ and ξ^2 of the form, $y = b + mx$ as follows:

$$e_t\ (1 + K^2 \xi^2) = e_o + (K \chi)\ \xi^2 \tag{25}$$

Since the strains are limited to the elastic region, Hooke's Law may be applied to give

$$\sigma_t = E\, e_t$$

$$\sigma_t = E\, \frac{e_o + K\chi\xi^2}{1 + K^2\xi^2} \tag{26}$$

Eqn. (26) substituted into eqns. (16) and (17) produces

$$P = 2ahE \int_o^1 \frac{(e_o + K\chi\xi^2)(1 - \tau K^2\xi^2)}{(1 + K^2\xi^2)^2}\, d\xi \tag{27}$$

$$T = 2a^2hE \int_o^1 \frac{K\xi^2(e_o + K\chi\xi^2)(1 - \tau K^2\xi^2)}{(1 + K^2\xi^2)^2}\, d\xi \tag{28}$$

Non-dimensionalizing these expressions there is

$$P^* = \frac{P}{2ahE}$$

$$P^* = e_o \int_o^1 \frac{1 - \tau K^2\xi^2}{(1 + K^2\xi^2)^2}\, d\xi + \chi \int_o^1 \frac{K\xi^2 - \tau K^3\xi^4}{(1 + K^2\xi^2)^2}\, d\xi \tag{29}$$

$$T^* = \frac{T}{2a^2hE}$$

$$T^* = e_o \int_o^1 \frac{K\xi^2 - \tau K^3\xi^4}{(1 + K^2\xi^2)^2}\, d\xi + \chi \int_o^1 \frac{K^2\xi^4 - \tau K^4\xi^6}{(1 + K^2\xi^2)^2}\, d\xi \tag{30}$$

Eqns. (29) and (30) are the fundamental theoretical equations to be solved. The various integrals are constants determined by the non-dimensional rate of twist, K, and are redefined as α coefficients so that

$$P^* = \alpha_{11} e_o + \alpha_{12} \chi \tag{31}$$

$$T^* = \alpha_{21} e_o + \alpha_{22} \chi \tag{32}$$

where $\alpha_{12} = \alpha_{21}$.

These expressions can be inverted to solve for e_o and χ.

$$e_o = \frac{\alpha_{22}}{\alpha_{11}\alpha_{22} - \alpha_{12}^2} P^* + \frac{-\alpha_{12}}{\alpha_{11}\alpha_{22} - \alpha_{12}^2} T^* \tag{33}$$

$$\chi = \frac{-\alpha_{21}}{\alpha_{11}\alpha_{22} - \alpha_{12}^2} P^* + \frac{\alpha_{11}}{\alpha_{11}\alpha_{22} - \alpha_{12}^2} T^* \tag{34}$$

The coefficients of P* and T* in these equations are also constants and are redefined as β coefficients. Hence

$$e_o = \beta_{11} P^* + \beta_{12} T^* \tag{35}$$

$$\chi = \beta_{21} P^* + \beta_{22} T^* \tag{36}$$

where $\beta_{12} = \beta_{21}$.

Solving for the α coefficients in terms of β coefficients gives

$$\alpha_{11} = \frac{\beta_{22}}{\beta_{11}\beta_{22} - \beta_{12}\beta_{21}}$$

$$\alpha_{12} = \frac{-\beta_{12}}{\beta_{11}\beta_{22} - \beta_{12}\beta_{21}}$$

$$\alpha_{21} = \frac{-\beta_{21}}{\beta_{11}\beta_{22} - \beta_{12}\beta_{21}}$$

$$\alpha_{22} = \frac{\beta_{11}}{\beta_{11}\beta_{22} - \beta_{12}\beta_{21}} \qquad (37)$$

Eqns. (35) and (36) give e_o and χ for any combination of applied P* and T* if membrane theory alone adequately defines what is taking place. This solution will contain an appreciable error if the bending stresses, which the theory assumes to be zero, are of sufficient magnitude. Any such stresses would have a negligible component in the direction of the applied tensile load but they may constitute a significant portion of the torsional component. If it is assumed that bending stresses have a negligible effect on P*, membrane theory alone will adequately describe P* as in eqn. (31). If the cross-coupling coefficients, α_{12} and α_{21}, retain their equality in eqns. (31) and (32), then the only significant departure from membrane theory would be evident in α_{22}.

Assuming α_{11}, α_{12}, and α_{21} are all constants as determined by membrane theory, a different theoretical basis is chosen for evaluating α_{22}.

From eqns. (34) and (36) there is

$$\beta_{22} = \frac{\alpha_{11}}{\alpha_{11}\alpha_{22} - \alpha_{12}^2} \qquad (38)$$

α_{22} can be written as

$$\alpha_{22} = \frac{\alpha_{11}\alpha_{22} - \alpha_{12}^2 + \alpha_{12}^2}{\alpha_{11}}$$

$$\alpha_{22} = \frac{1}{\beta_{22}} + \frac{\alpha_{12}^2}{\alpha_{11}} \qquad (39)$$

In the theory of torsion for prismatic bars of narrow rectangular cross section the angular deformation is related to the applied torque by[1]

$$\frac{\psi'}{T} = \frac{1}{Gh^3(.667a - .21h)} \qquad (40)$$

A recent investigation by Chen Chu[2] has modified this relationship by a factor, f, so that it applies to rectangular bars with an initial twist.

$$\frac{\psi'}{T} = \frac{1}{fGh^3(.667a - .21h)} \qquad (41)$$

where

$$f = 1 + \frac{2}{15}(1+\mu)\left(\phi_{max}\frac{2a}{h}\right)^2 \qquad (42)$$

[1]Timoshenko, S., and J. N. Goodier, Theory of Elasticity (New York: McGraw-Hill Book Company, 1951) p. 278.

[2]Chen Chu, The Effect of Initial Twist on the Torsional Rigidity of Thin Prismatical Bars and Tubular Members, Proceedings of the First U. S. National Congress of Applied Mechanics, (New York: The American Society of Mechanical Engineers, 1952) p. 265.

Non-dimensionalizing eqn. (41) there is

$$\frac{\chi}{T^*} = \frac{2a^3E}{Gh^2(.667a - .21h)\left[1 + \frac{2}{15}(1+\mu)\left(\phi_{max}\frac{2a}{h}\right)^2\right]} \qquad (43)$$

For the condition of zero applied tensile load in eqn. (36),

$$\beta_{22} = \frac{\chi}{T^*} \qquad (44)$$

Eqn. (43) is therefore an expression for β_{22} based on the theory of torsion. Since this relationship is for a <u>rectangular</u> cross section, a slight modification of the h term is in order for the present case. As a first approximation it is assumed that the average blade thickness normal to the z-axis, h_{avg}, may be substituted.

$$h_{avg} = \int_0^1 \frac{t}{\cos\phi}\, d\xi \qquad (45)$$

$$h_{avg} = \int_0^1 h(1 - \tau K^2 \xi^2)\, d\xi = h\left(1 - \frac{\tau K^2}{3}\right) \qquad (46)$$

Substituting into eqn. (39), α_{22} is found to be

$$\alpha_{22} = \frac{Gh_{avg}^2(.667a - .21h_{avg})\left[1 + \frac{2}{15}(1+\mu)\left(\phi_{max}\frac{2a}{h_{avg}}\right)^2\right]}{2a^3E} + \frac{\alpha_{12}^2}{\alpha_{11}} \qquad (47)$$

This establishes the last unknown influence coefficient in eqns. (31) and (32), allowing a complete determination of these equations as well as eqns. (35) and (36). These equations now completely describe

the deformation of a twisted blade under any combination of applied tensile load and torque, within the range of validity of the previously listed assumptions.

3. Test Equipment and Procedures.

Purpose

The purpose of testing was to obtain experimental data for longitudinal and angular deformations for known values of applied torque and tensile load utilizing blades of different initial twist rates. From these relationships experimental values were available for:

a. Young's Modulus, E.

b. The strain distribution across the chord for comparison with the parabolic distribution predicted by eqn. (25).

c. β coefficients in eqns. (35) and (36) for comparison with the theoretical values.

Background

The basic requirement for testing a twisted blade under the conditions described in the Analysis is to have a test apparatus which allows the application of arbitrary, but known, external tensile loads and moments. Lacking any such apparatus, tests were devised to investigate the two extreme situations:

Test I: An applied axial load with no applied moment.

Test II: An applied moment with no applied axial load.

Test Specimens

Test I can not be accomplished in a normal tensile test since any tendency for the blade to untwist in reaction to applied tension would be resisted by the gripping head, thus introducing an undesired applied

torque of unknown magnitude. Even a "swivel" head would tend to introduce such a torque due to the large frictional forces involved. For this reason the test specimen was machined to twist in one direction over half the length of the specimen and then the twist was reversed over the other half. These halves were therefore symmetrical except for the reversed twist. Any tendency for one half to untwist under tension was exactly equal to that of the other half. The center of the specimen was then free to untwist and, since one twisted section had no effect on the other, each half was essentially a twisted blade in tension but free of applied torque.

The test specimens were machined with a 1.25 inch diameter cutting bit from one and one-half inch diamater 7075-T6 extruded aluminum rod. The design was such that a cross section normal to the z-axis was essentially a rectangle of width h = .2 inches and length 2a = 1.5 inches. Thus $\gamma = R/h = 3.125$.

Three different test specimens were machined, as shown in Fig. 4. The machined twist, as characterized by dO/dz, was 22.5, 11.25, and zero degrees per inch for specimens #1, #2, and #3 respectively. At the center of specimens #1 and #2, prior to reversing the twist, a short section of the rod was left intact to allow for the measurement of the deformation twist, ψ. The twisted sections were approximately nine inches long so that strain readings taken at the midsection would be free of end effect.

Longitudinal Deformation

Longitudinal deformations were measured by means of strain gages, type FAP 12-12 (S13) and type A-7, bonded to the specimen at the center of each machined section. Placement was such that strains along the tangent to the helix were obtained at ξ = 0, 1/2, 3/4, and 1 on each side/edge of the blade. This duplicate placement plus the "double-ended" feature of the two twisted specimens allowed for a good multiplicity of data.

The strain gages were fed through a 20 channel Baldwin-Lima-Hamilton Switching and Balancing Unit and into a Budd DATRAN Digital Strain Indicator, shown in Fig. 5. This arrangement combined the advantages of a direct strain reading in micro inches per inch with a rapid reading capability on all gages.

Angular Deformations

If a circular disc of radius 11.46 inches were attached as a collar to the specimen, a radial angle of five degrees would subtend an arc length of one inch on the circumference of the disc. An angle indicator, shown in Fig. 6, was devised with this principle in mind. Rather than the complete disc, a three inch width of the disc was clamped around the specimen and the circumferential arc was calibrated in inches. A sighting gage fixed in a suitable stationary position then allowed circumferential linear readings for angular deflections. These readings of ψ, taken in sixteenths of an inch, were converted to χ by the multiplying factor

$$\chi = \left[\frac{5}{16} \cdot \frac{1}{57.3} \cdot \frac{a}{L} \right] \psi \qquad (48)$$

where L is the length of the twisted section.

Test I

Test I was conducted in a 300,000 pound Riehle Testing Machine. The specimen was positioned to accept a tensile load and gripped in fixed clamping heads at either end. The angle indicator was clamped between the two twisted sections for specimens #1 and #2, with the sighting gage appropriately placed to read instantaneous angular deformations. The test set-up is shown in Figs. 7 through 9.

The strain gages and angle indicator were zeroed at a preload of 1000 pounds, referred to as "gage zero". Readings were taken at 2000 pound intervals to 10,000 pounds gage. This range of loads allowed the maximum strain to remain well below the elastic limit of the material.

Test II

Test II was a torsion test with P = 0. For this test a torsional apparatus was set up as shown in Figs. 10 through 12. The twisted specimens were clamped at the center section and supported at the free end by an idler, in which the specimen was free to rotate. Also attached at the free end was the angle indicator and a moment arm. The moment arm was designed to act as a ten inch lever when loads were applied at a right angle to it through the eye bolt. A cable attached to the eye bolt fed through a dynamometer and pulley arrangement to a take-up ratchet. In this manner the applied moment was simply the dynamometer reading multiplied by the ten inch lever arm.

As in Test I, an initial load was applied and all gages zeroed. Readings of strain, angular deformation, and applied torque were then taken in increments of applied torque.

4. Results and Discussion.

The experimental value of Young's Modulus, as determined from Fig. 13 and Hooke's Law, was $E = 10.1 \times 10^6$ psi. This is two percent lower than the handbook value[1] for the test material but was considered to be the most accurate figure available for that material sample. The experimental E and the handbook values for the shear modulus, G,[2] and Poisson's ration, μ ,[3] were used as material constants in all calculations. An experimental value for the shear modulus could have been determined by a torsional test on the round stock prior to machining. From this test the shear modulus could be found from the torsional relationship for circular rods,

$$\psi' = \frac{T}{JG}$$

where J is the polar moment of inertia. The absence of such a test was an oversight in the test procedure.

Table I lists the α and β coefficients for each of the three specimens, comparing the theoretical values with those determined by test. A graphical comparison of theoretical and experimental values

[1] United States Department of Defense, Strength of Metal Aircraft Elements: Military Handbook 5 (Washington: Government Printing Office, 1955) p. 114.

[2] Ibid.

[3] Eshbach, O. W., Handbook of Engineering Fundamentals (New York: John Wiley & Sons, 1965) p. 12-56.

of the various coefficients relative to the initial twist rate is plotted in Fig. 14. It is significant to note the rather good degree of correlation attained by a relatively simple theory. The cross coupling coefficients, α_{12} and α_{21}, β_{12} and β_{21}, were found to be equal as the analytical solution predicted. Preliminary investigation made it clear that membrane theory alone produced extremely erroneous values for α_{22}. The modification introduced in the Analysis to obtain α_{22} from a theoretical β_{22} based on the theory of torsion proved to allow a reasonable prediction of this coefficient. It should be noted here that an error was introduced in the application of Chen Chu's modifying factor for the high initial rate of twist since he stated that there was an upper limit in his analysis, beyond which higher order effects were significant. [1] This upper limit corresponds to the initial twist of Specimen #2.

TABLE I

TABULATION OF RESULTS

Coefficient	Specimen #1 K = .2945		Specimen #2 K = .1473		Specimen #3 K = 0	
	Theory	Test	Theory	Test	Theory	Test
11	.866	.892	.963	.947	1.0	.980
12	.0749	.0668	.0460	.0389	0	0
21	.0749	.0696	.0460	.0396	0	0
22	.0204	.0169	.0121	.0115	.00838	.00897
11	1.69	1.62	1.27	1.23	1.0	1.02
12	-6.21	-6.40	-4.82	-4.16	0	.08
21	-6.21	-6.67	-4.82	-4.24	0	0
22	71.8	85.5	101.0	101.3	119.3	111.4

The three experimental values of β_{11} were obtained from Fig. 15, where e_o versus P* is plotted for T* = 0 (Test I). The other coefficient obtainable from Test I was β_{21}, the ratio of χ to P* with T* = 0. These values were obtained from Fig. 16. Likewise, Test II provided experimental determination for coefficients β_{12} and β_{22}, $(e_o/T^*)_{P^*=0}$ and $(\chi/T^*)_{P^*=0}$, respectively, as obtained from Figs. 17 and 18. These β coefficients were converted to experimental α coefficients by eqn. (37).

Figs. 19, 20, and 13 are plots of strain data obtained from Test I for Specimens #1, #2, and #3 respectively. The strain reading from every station, modified by the factor $(1 + K^2\xi^2)$, was plotted versus ξ^2 for P = 10,000 pounds, T = 0. This strain distribution across the chord is seen to plot in a linear fashion as predicted by eqn. (25), which is drawn as the solid line. Since the tangential strain at all chordwise stations was found to vary linearly with load, the value of 10,000 pounds was simply a convenient basis and any other load would plot qualitatively the same.

The strain distribution over the chord was essentially parabolic for twisted specimens, with the greatest strain realized at the midpoint of the chord. The strain relief evident at the outer fibers is directly attributable to the amount of angular deformation, or "unwinding" of these specimens. An interesting point to note in Fig. 19 is that while the specimen is subjected to a 10,000 tensile load, the outer fibers are actually in compression. This is a result of the extreme angular deformation for the case of high initial twist rate. For the untwisted specimen the strain distribution was uniform over the chord, as one would expect.

Figs. 21 through 23 are similar plots of strain distribution across the chord but for the condition T $\cong$ 125 inch pounds, P = 0. Again the parabolic nature of the strain distribution is evident from the data for the twisted specimens, but there is no discernible pattern for the untwisted specimen. This last case appeared to be the only test in which the measured surface strain was not representative of the actual strain at the central fibers at each station. The "back to back" arrangement of strain gages on all specimens served as a check for this type of discrepancy. Test II of Specimen #3 was the only case in which a noticeable difference in strain readings was found from one side of the blade to the other. These differences were qualitative as well as quantitative, with e_o actually changing from tension to compression from one surface to the other. Even an average of each "back to back" pair of strain gages failed to provide a discernible pattern of behavior for this specimen.

The reason for the lack of conformity of this test can most likely be traced to the test apparatus. The torsion idler ideally allowed the specimen to rotate completely free of friction but, at the same time, completely supported in all directions so no bending normal to the z-axis would occur. A compromise was adopted for this item in that the idler was simply a block support with a slightly oversize hole to allow free rotation. The resulting "play" in this hole allowed some degree of bending of all specimens as the moment was applied, but only in the case of Specimen #1, where the magnitudes of longitudinal strains due to torsion were so small, did the longitudinal strains due to bending become an important factor.

The untwisted specimen, of course, violates the assumption of "large" initial twist rates that was made in the analysis of membrane stresses. However, at low rates of twist the membrane stresses become insignificant in comparison with the shearing stresses in resisting an applied moment. The untwisted specimen was therefore included in the test as an important limiting case. It also served as a means of experimentally determining Young's Modulus.

The results of these tests have shown the theoretical approach herein utilized to be a good first approximation for defining the reaction of a twisted blade to a combined stress field. The results are not exhaustive, however, since specimens of many different initial twist rates and cross sectional aspect ratios would be required to establish a definitive pattern of response. An ability to apply completely arbitrary combinations of load and moment in the test procedure would provide for a more thorough investigation of experimental-theoretical correlation.

Second order effects which were neglected in this analysis assume much more importance at very low initial twist rates. It is assumed that membrane theory would prove more reliable for a thinner blade cross section; i.e., as the blade actually approached a pure membrane.

5. Conclusions.

The conclusions to be drawn from this paper are, for a twisted blade of narrow rectangular cross section:

a. Modified membrane theory provides a good first approximation to the response of the blade to combined loads of tension and torsion.

b. The strain distribution across the chord is essentially parabolic and is accurately predicted for the twisted specimens tested.

6. Recommendations.

It is recommended that further work in the area of twisted blades under combined loading be directed toward

a. a more complete theoretical treatment, to include, for example, a detailed analysis of the shear stresses in the plane of the cross section as well as an investigation of the effect of higher order terms that were neglected in the present analysis,

b. the development of an experimental apparatus that will allow a complete freedom of choice of combinations of the applied loads, and

c. a confirmation of the validity of the conclusions made in this paper by tests on a number of specimens in which both cross sectional aspect ratios and initial twist rates are varied.

7. Acknowledgements.

The advice of Professor J. E. Brock concerning the design of the test specimens is gratefully acknowledged. I am particularly indebted to Mr. Frank Abbe, whose mechanical ingenuity provided the means to machine all test specimens. The competent technical assistance in instrumenting the test specimens was furnished by Mr. Robert Besel. Above all, I thank my Advisor, Professor T. H. Gawain, for the initial suggestion of this topic and for his continued help and encouragement throughout the project.

BIBLIOGRAPHY

1. Chen Chu, The Effect of Initial Twist on the Torsional Rigidity of Thin Prismatical Bars and Tubular Members, Proceedings of the First U. S. National Congress of Applied Mechanics, The American Society of Mechanical Engineers, 1952.

2. Eshbach, O. W., Handbook of Engineering Fundamentals, 2nd ed., Wiley, 1952.

3. Timoshenko, S., and J. N. Goodier, Theory of Elasticity, 2nd ed., McGraw-Hill, 1951.

4. Todhunter, I., and K. Pearson, A History of the Theory of Strength of Materials, Vol. II, Dover Publications, 1960.

5. United States Department of Defense, Strength of Metal Aircraft Elements, Military Handbook 5, U. S. Government Printing Office, 1955.

6. Weast, R. C., Standard Mathematical Tables, 12th ed., The Chemical Rubber Company, 1959.

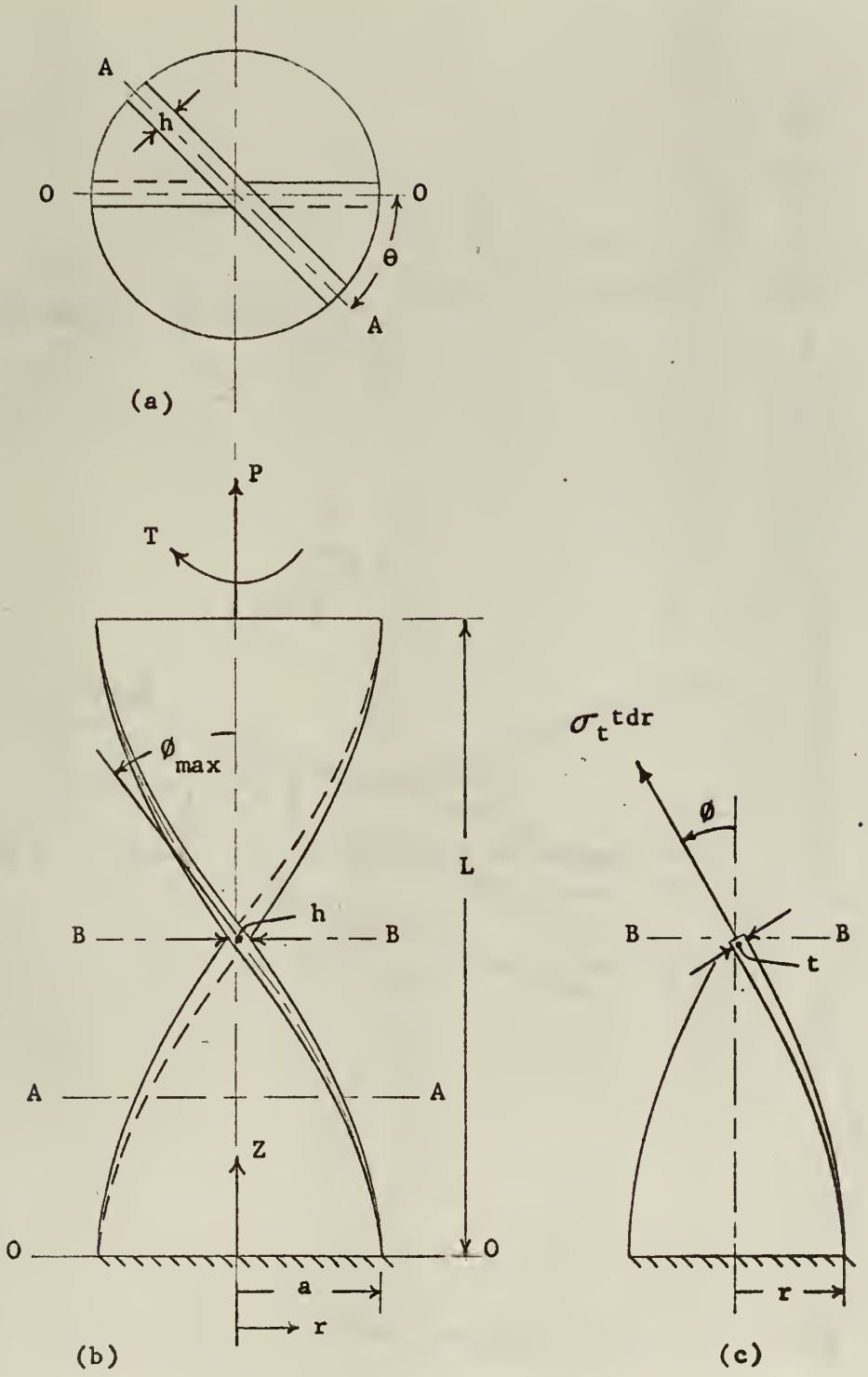

Fig. 1. Diagram of Analytical Model.

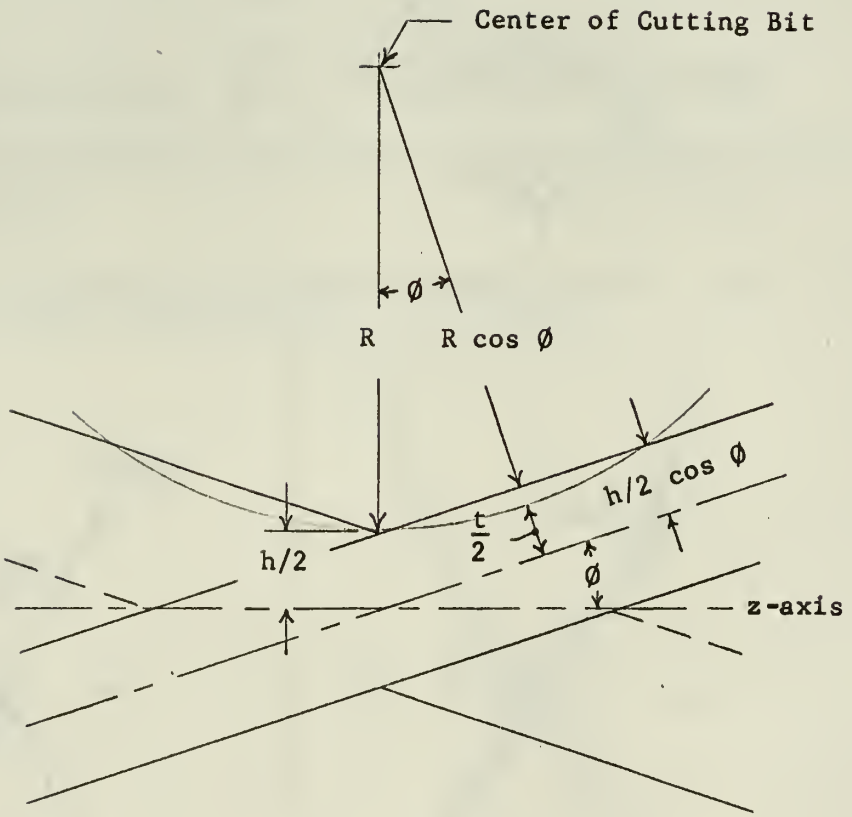

Fig. 2. The Blade Thickness, t.

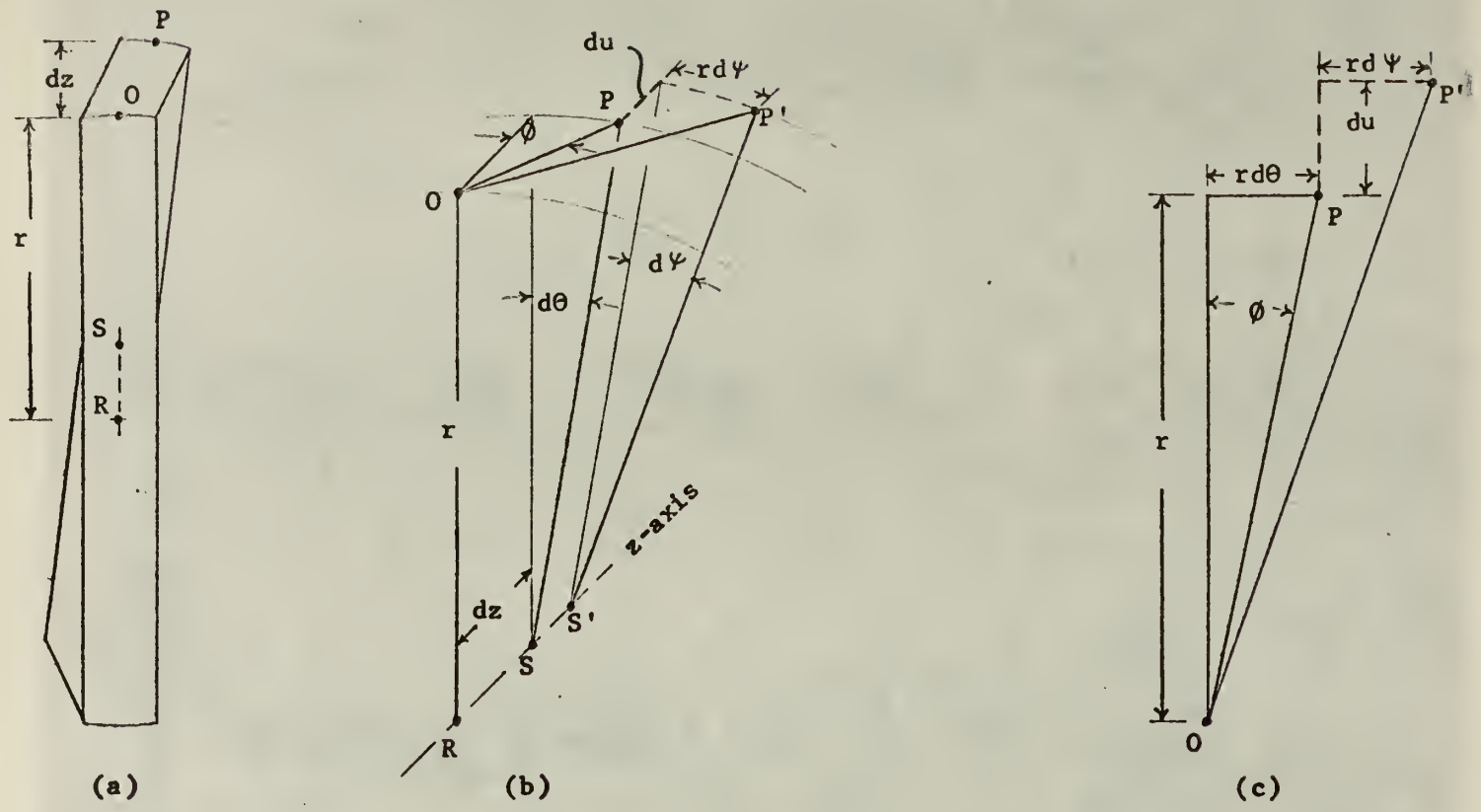

Fig. 3. Diagram of Elemental Length of Blade Showing Initial Condition (line OP) and Strained Condition (line OP').

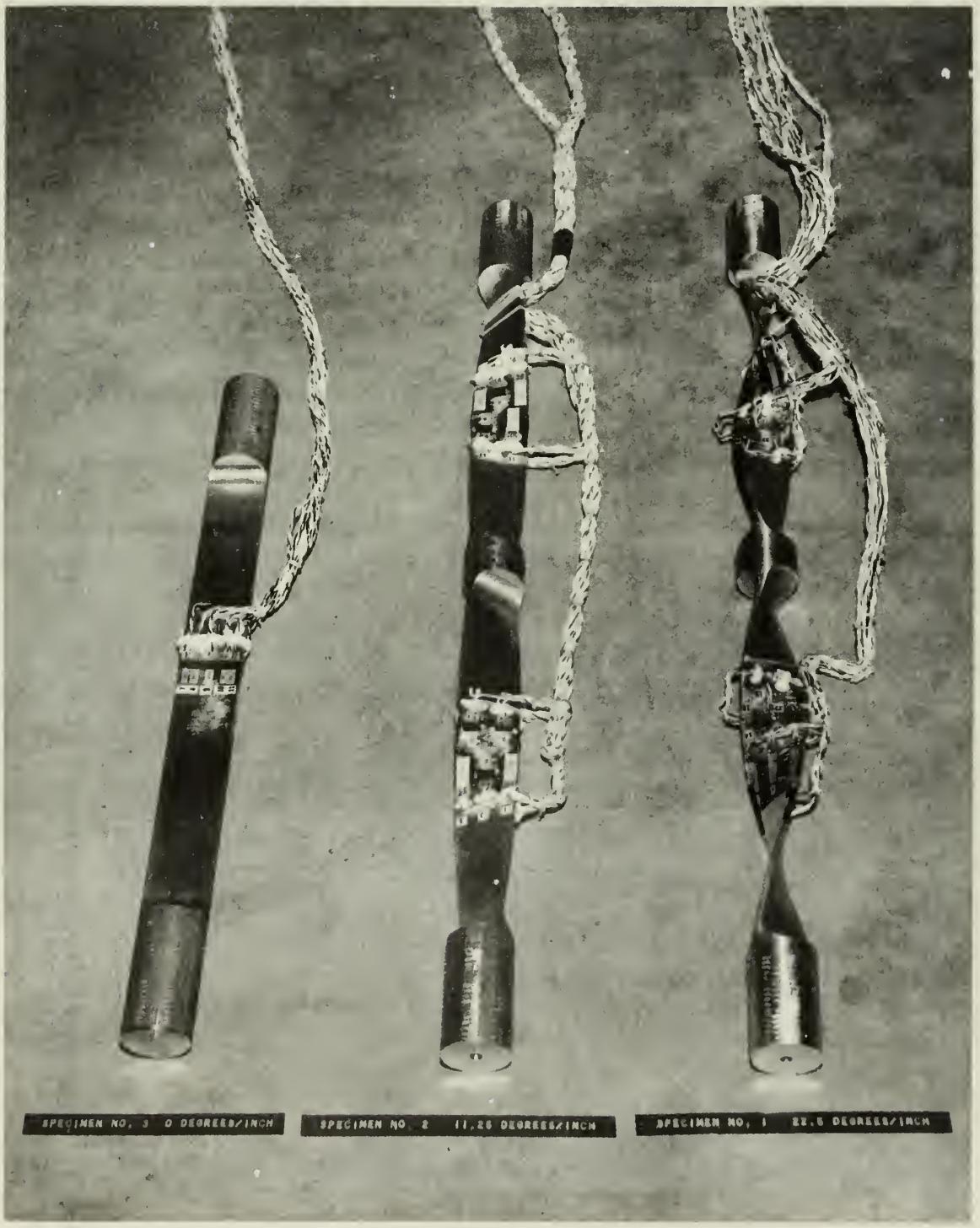

Fig. 4. The Test Specimens

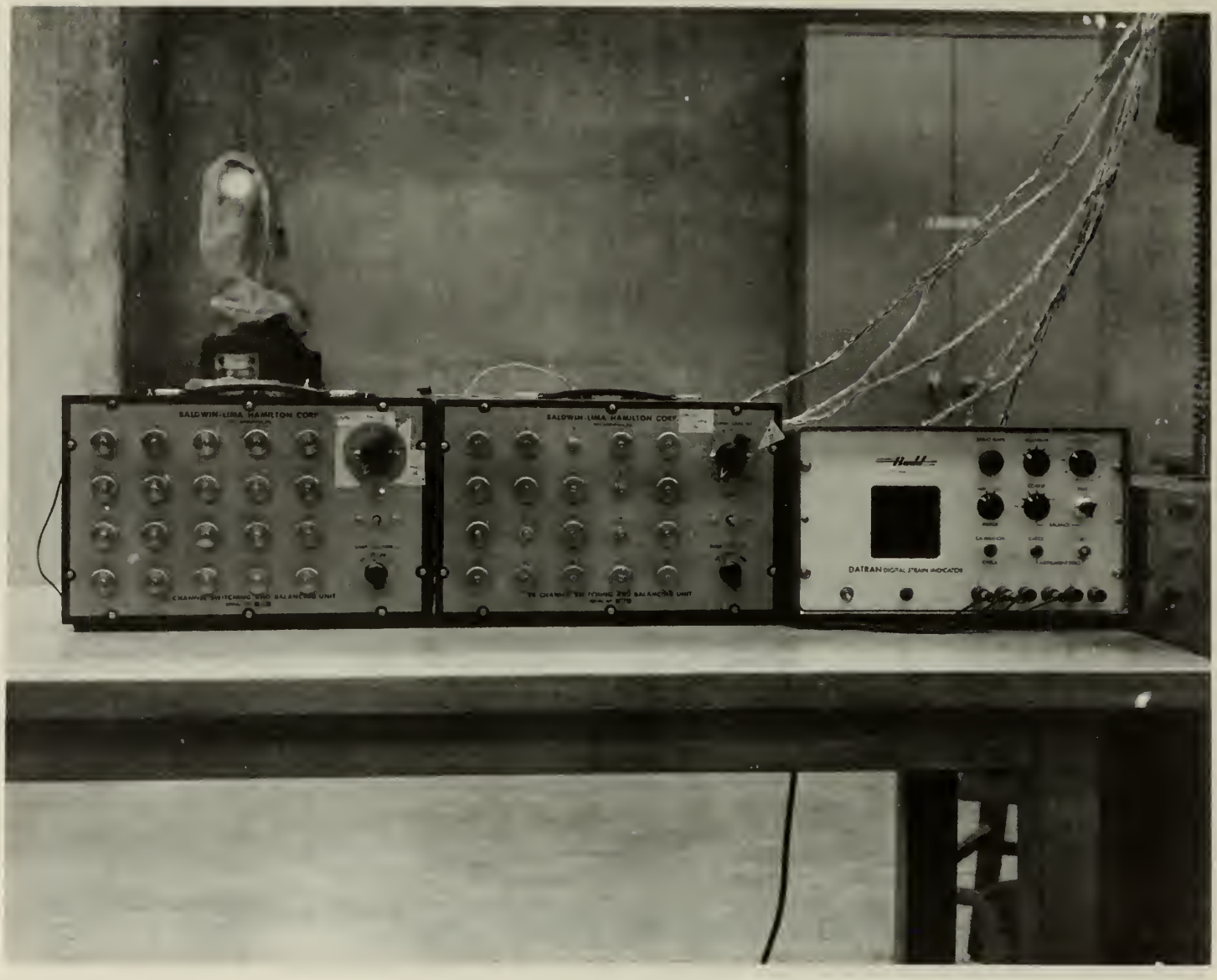

Fig. 5. BLH Switching and Balancing Unit and Budd DATRAN Digital Strain Indicator

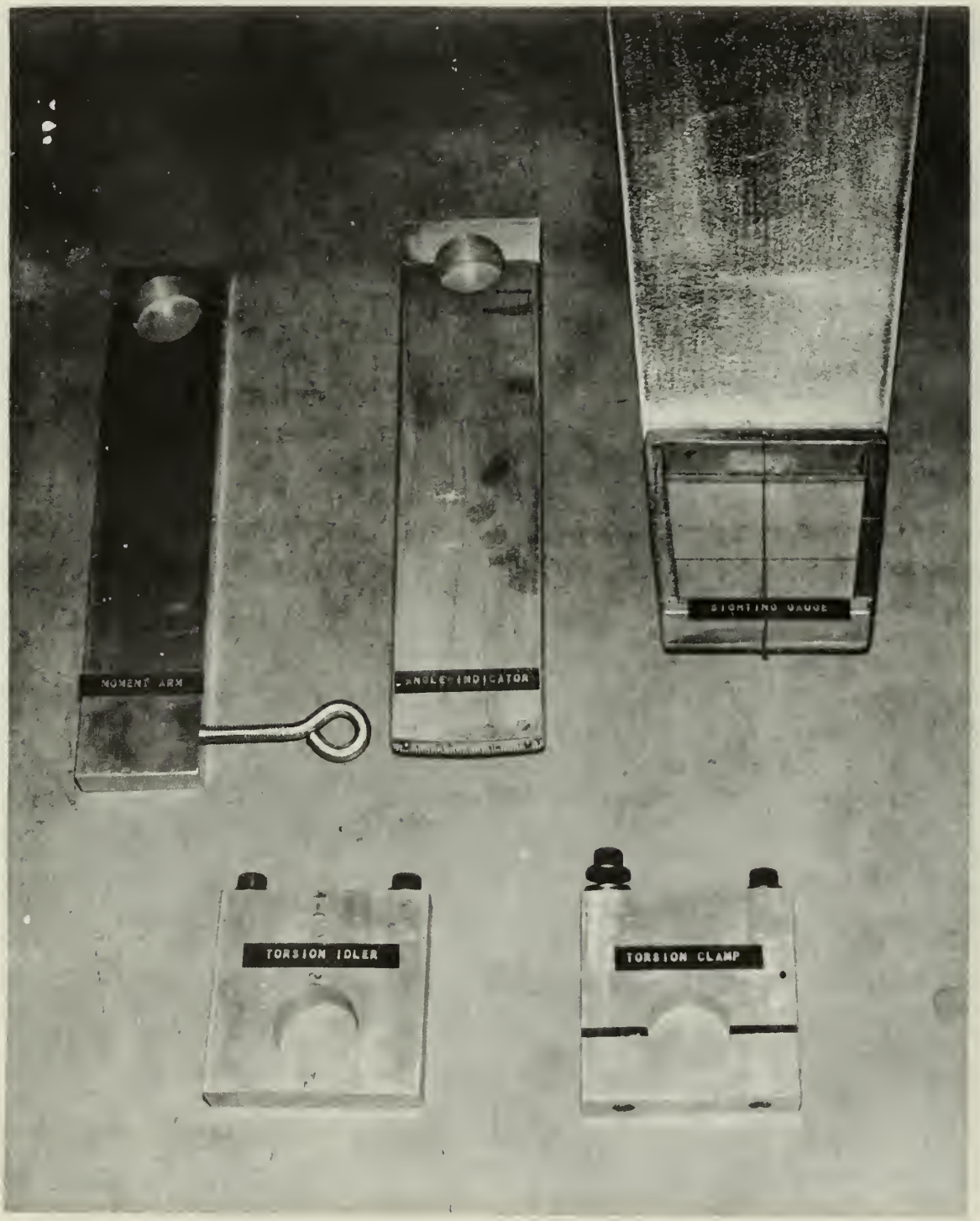

Fig. 6. Display of Experimental Apparatus

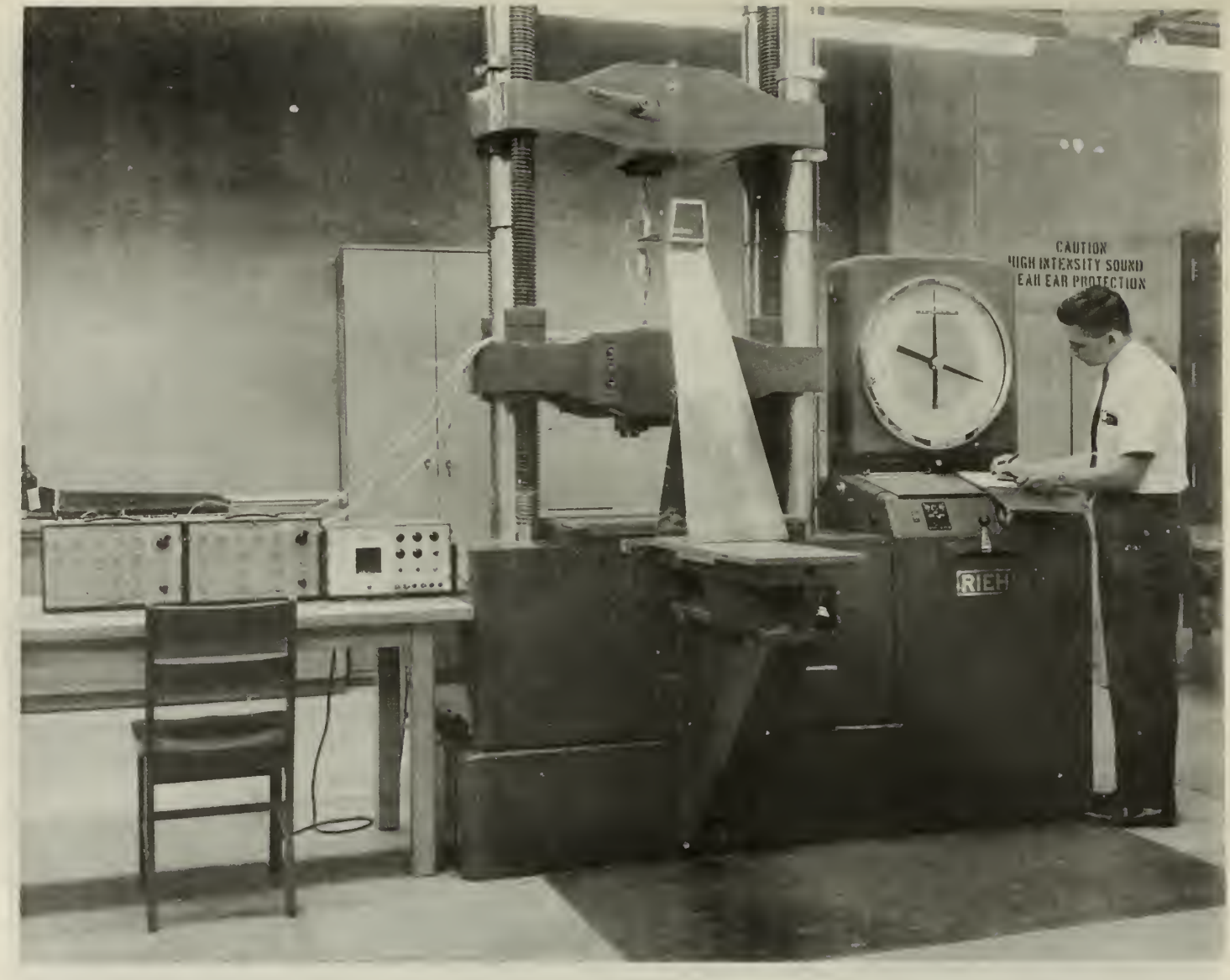

Fig. 7. Experimental Set-up, Test 1 (view a)

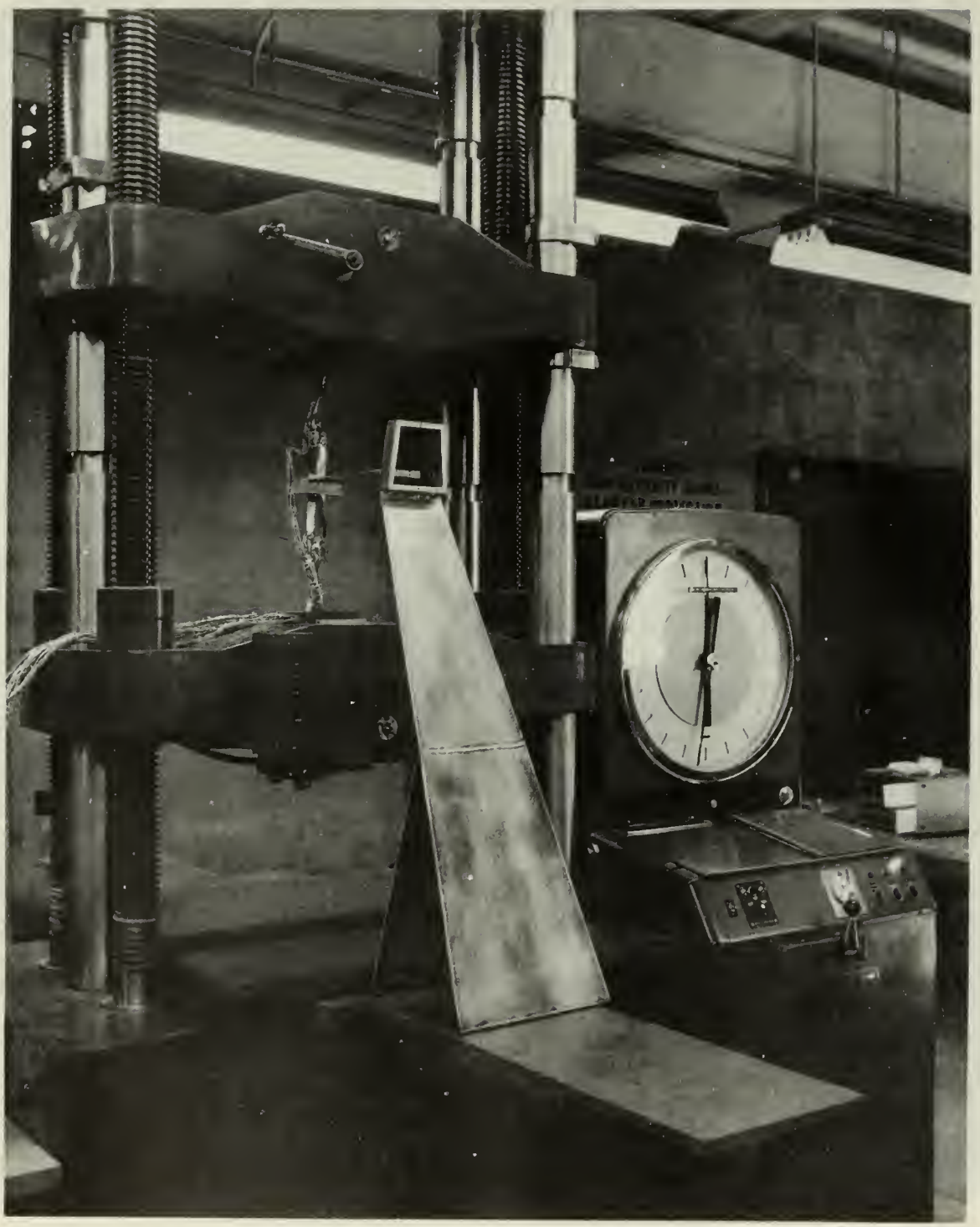

Fig. 8. Experimental Set-up, Test 1 (view b)

Fig. 9. Experimental Set-up, Test I (view c)

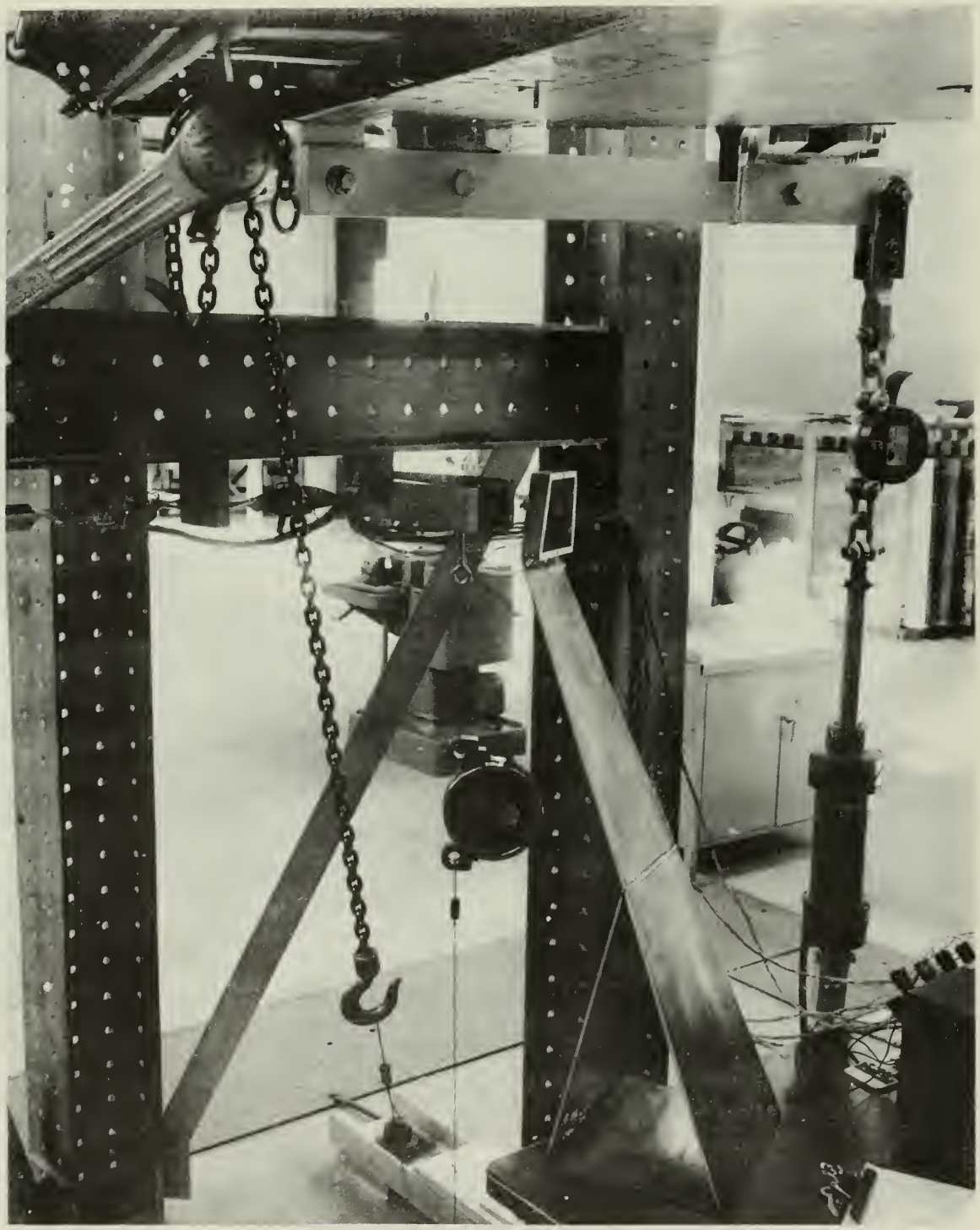

Fig. 10. Experimental Set-up, Test II (view a)

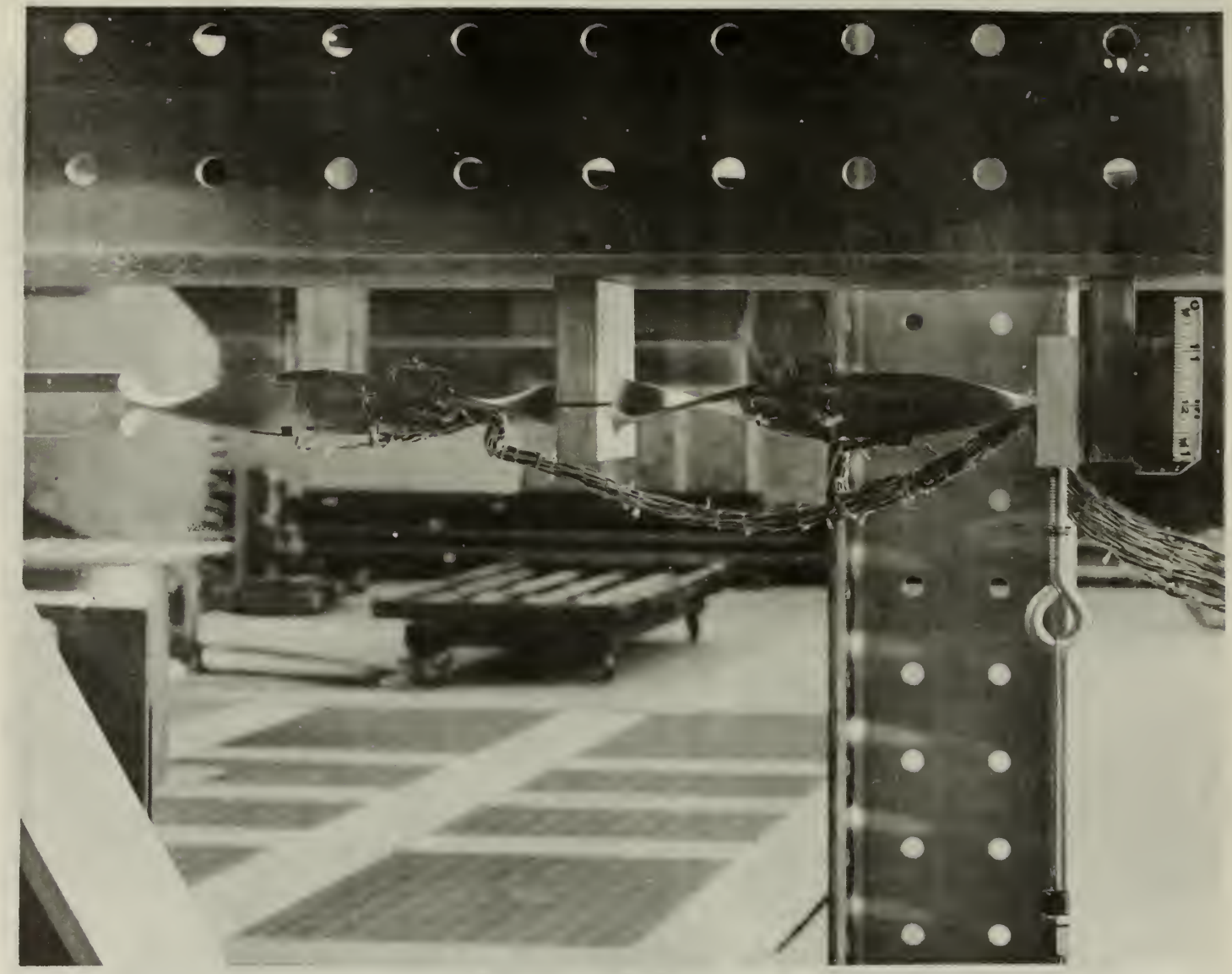

Fig. 11. Experimental Set-up, Test II (view b)

Fig. 12. Experimental Set-up, Test II (view c)

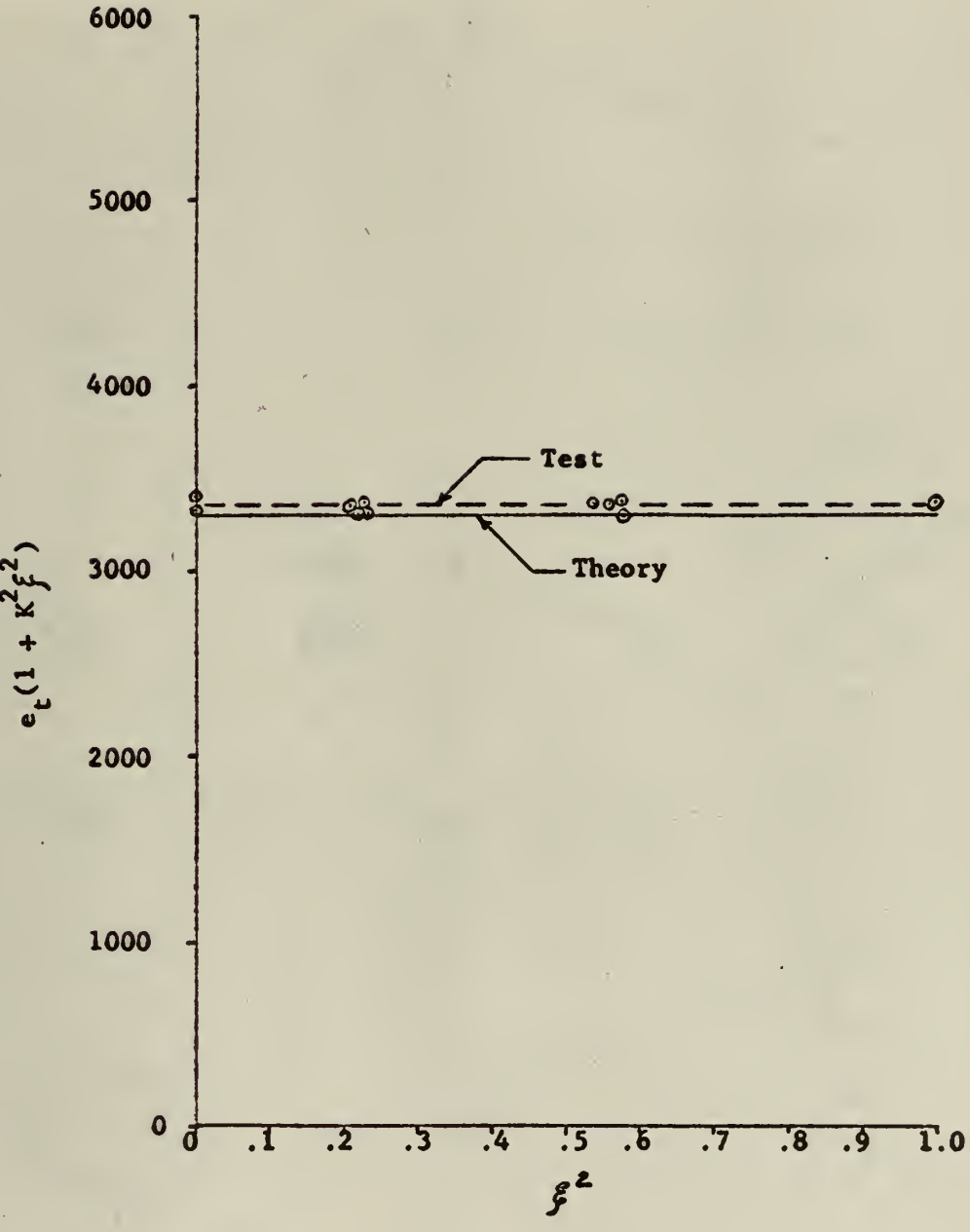

Fig. 13. Strain Distribution Across the Chord, Specimen #3, Test I (P = 10,000 pounds).

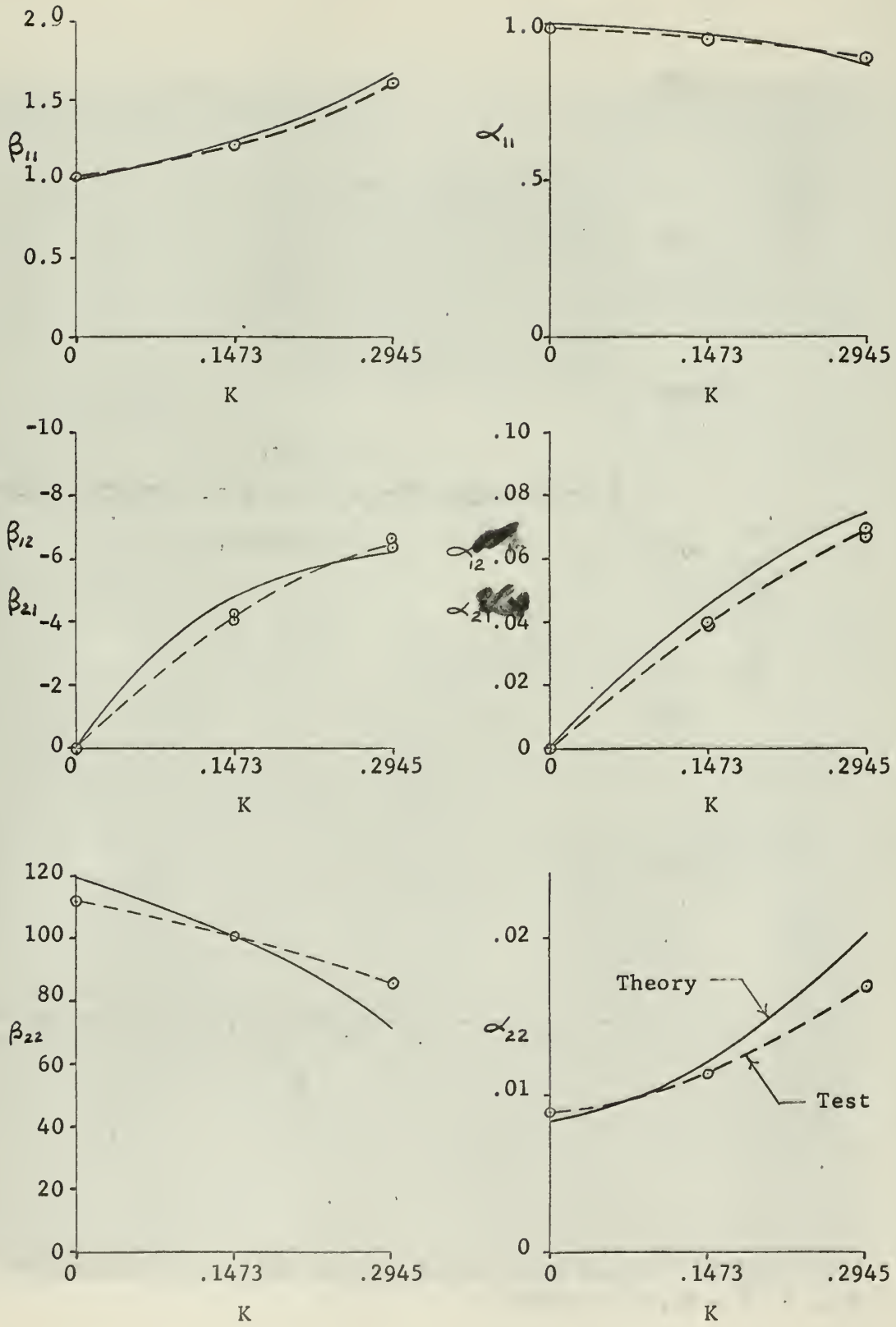

Fig. 14. Comparison of Theoretical and Experimental Values of α and β Coefficients Relative to Initial Twist Rate.

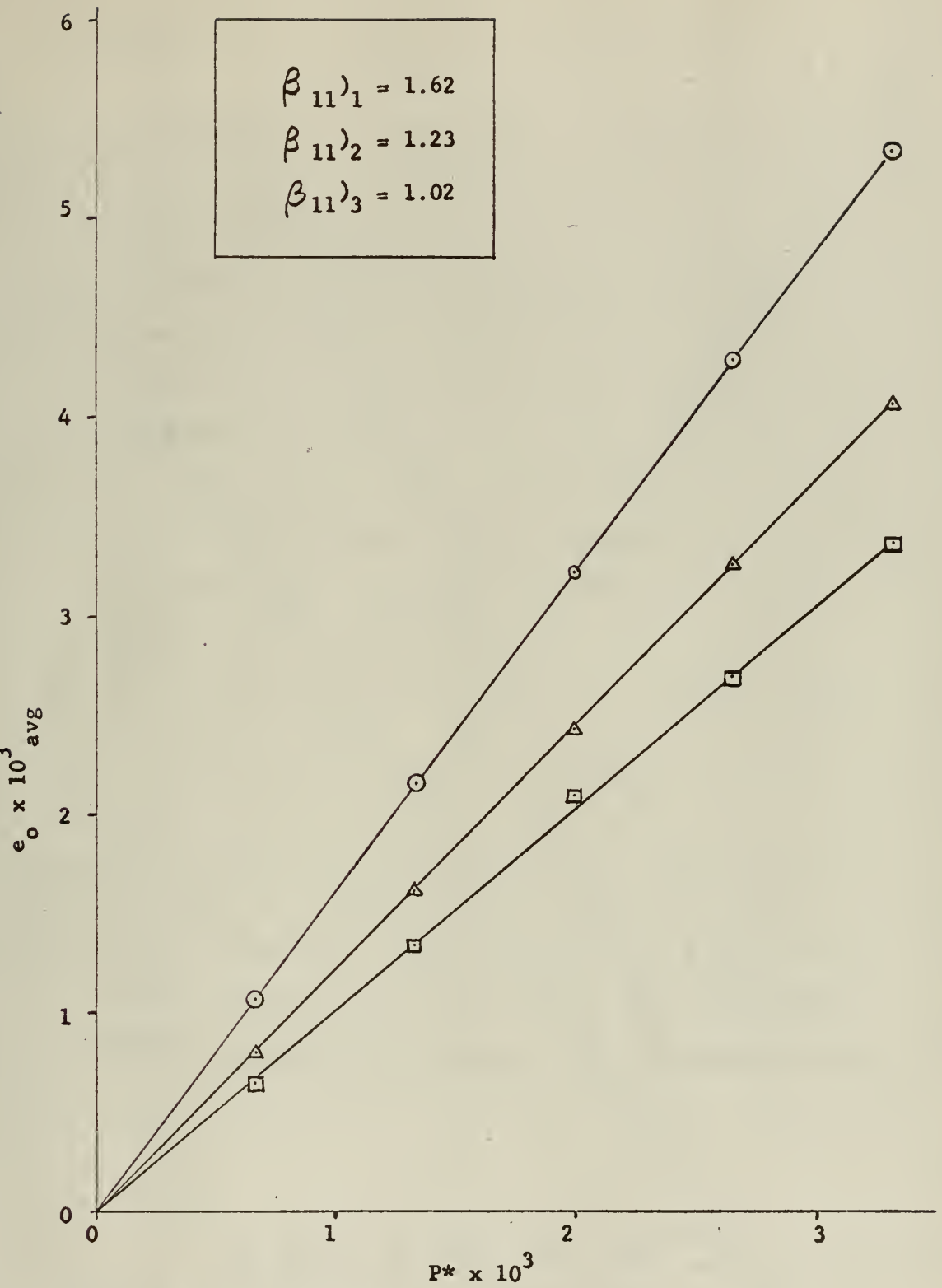

Fig. 15. Plot of $(e_o/P^*)_{T^*=0}$

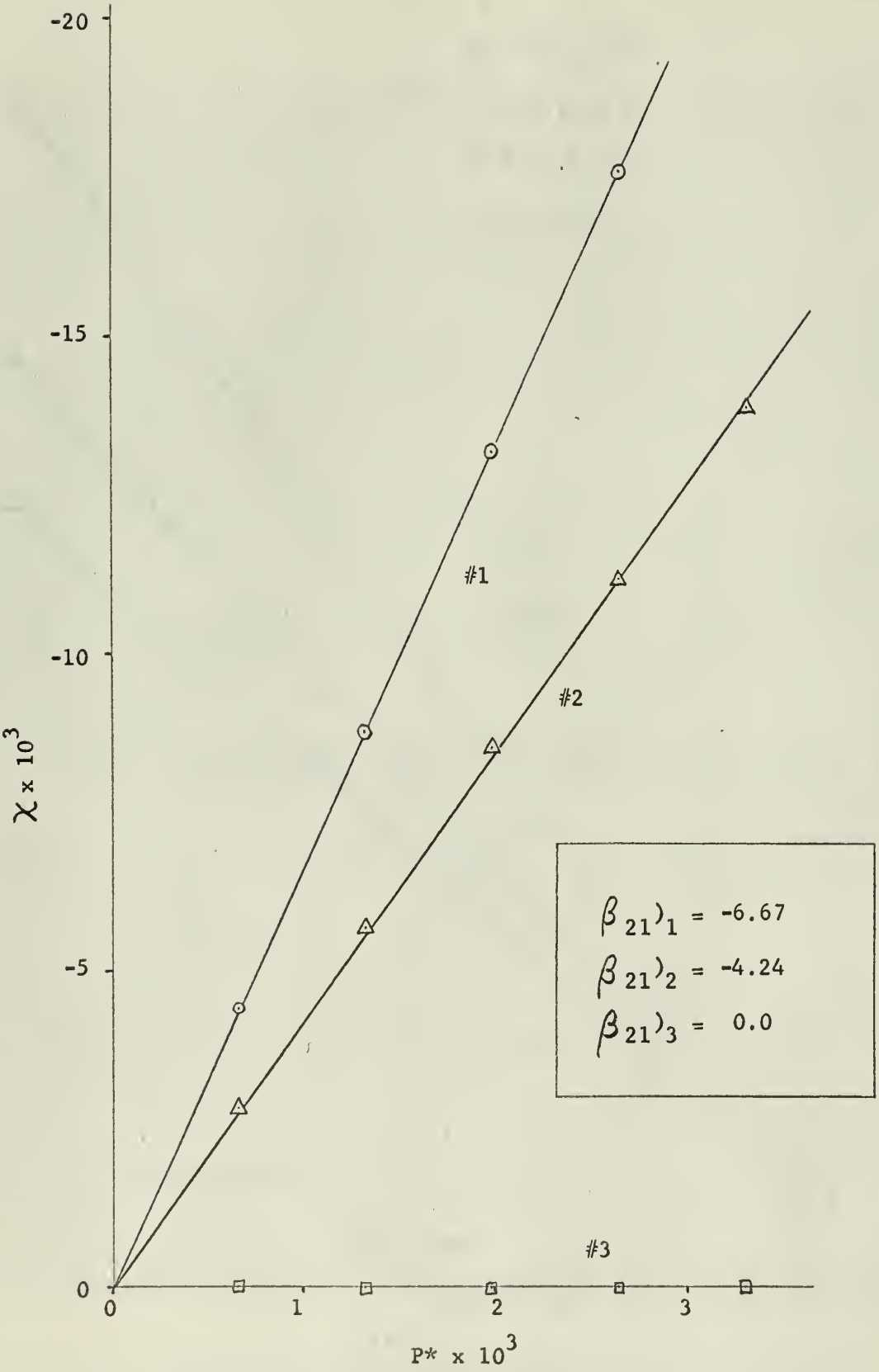

Fig. 16. Plot of $(\chi/P^*)_{T^*=0}$

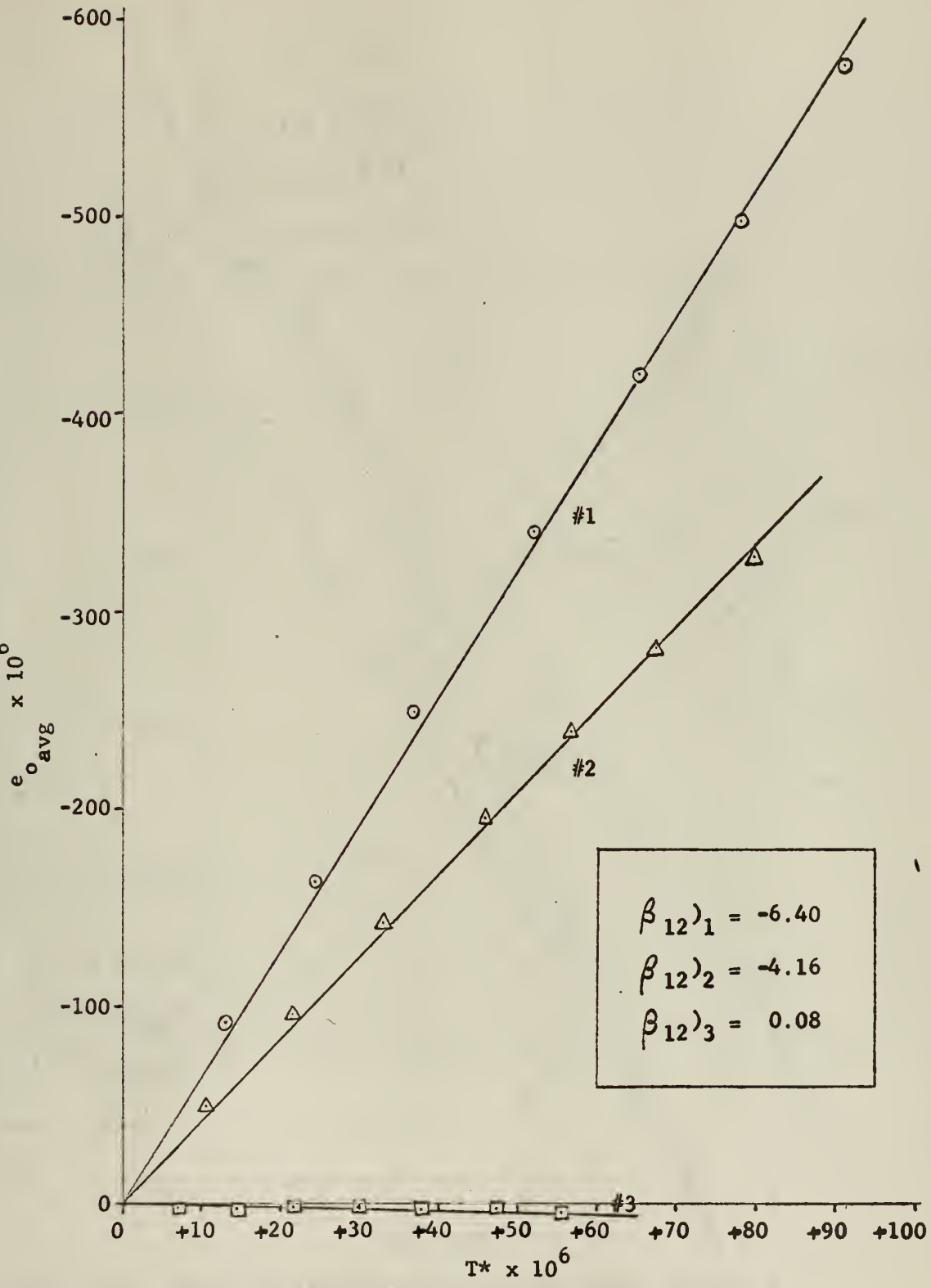

Fig. 17. Plot of $(e_o/T^*)_{P^*=0}$

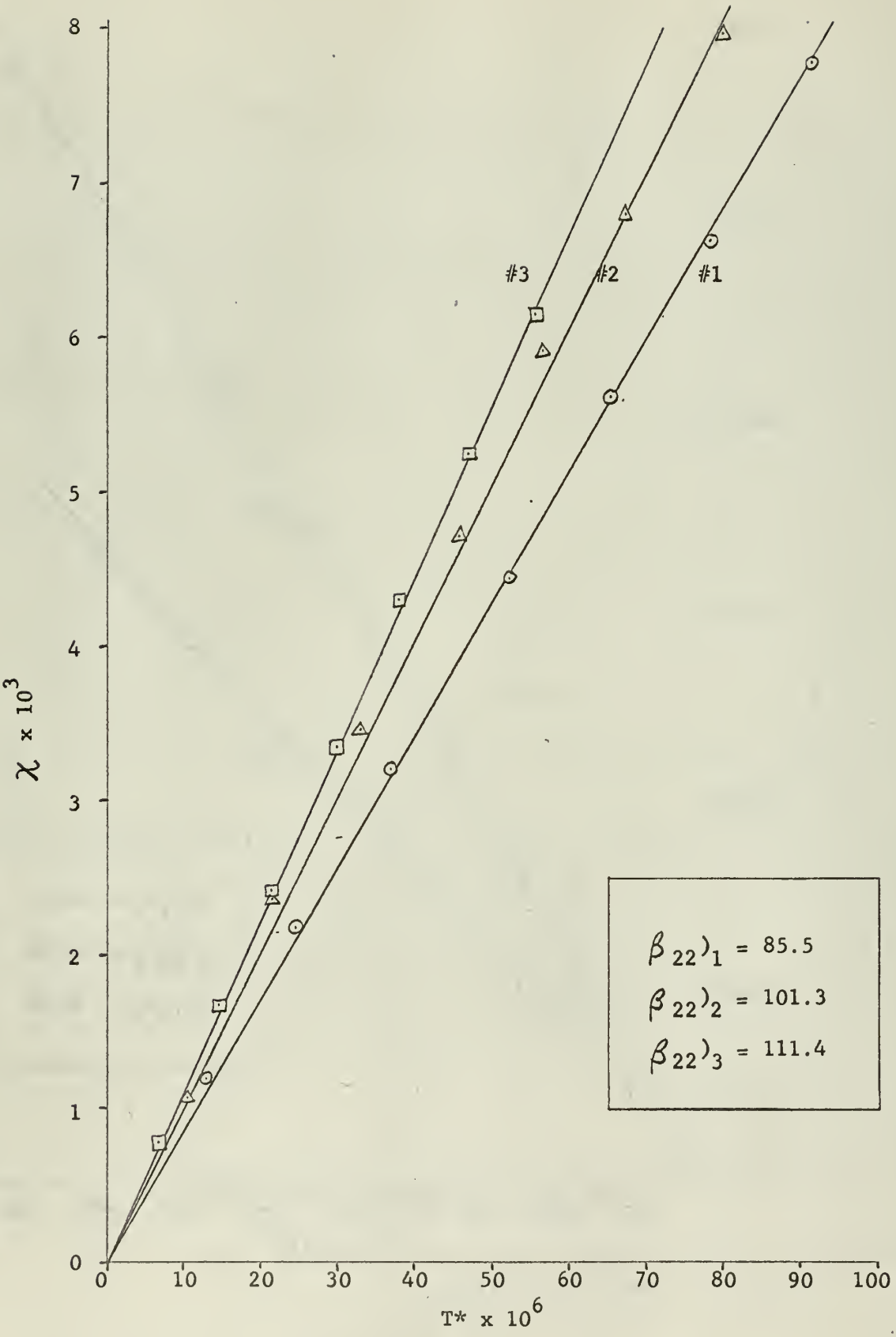

Fig. 18. Plot of $(\chi/T^*)_{P^*=0}$

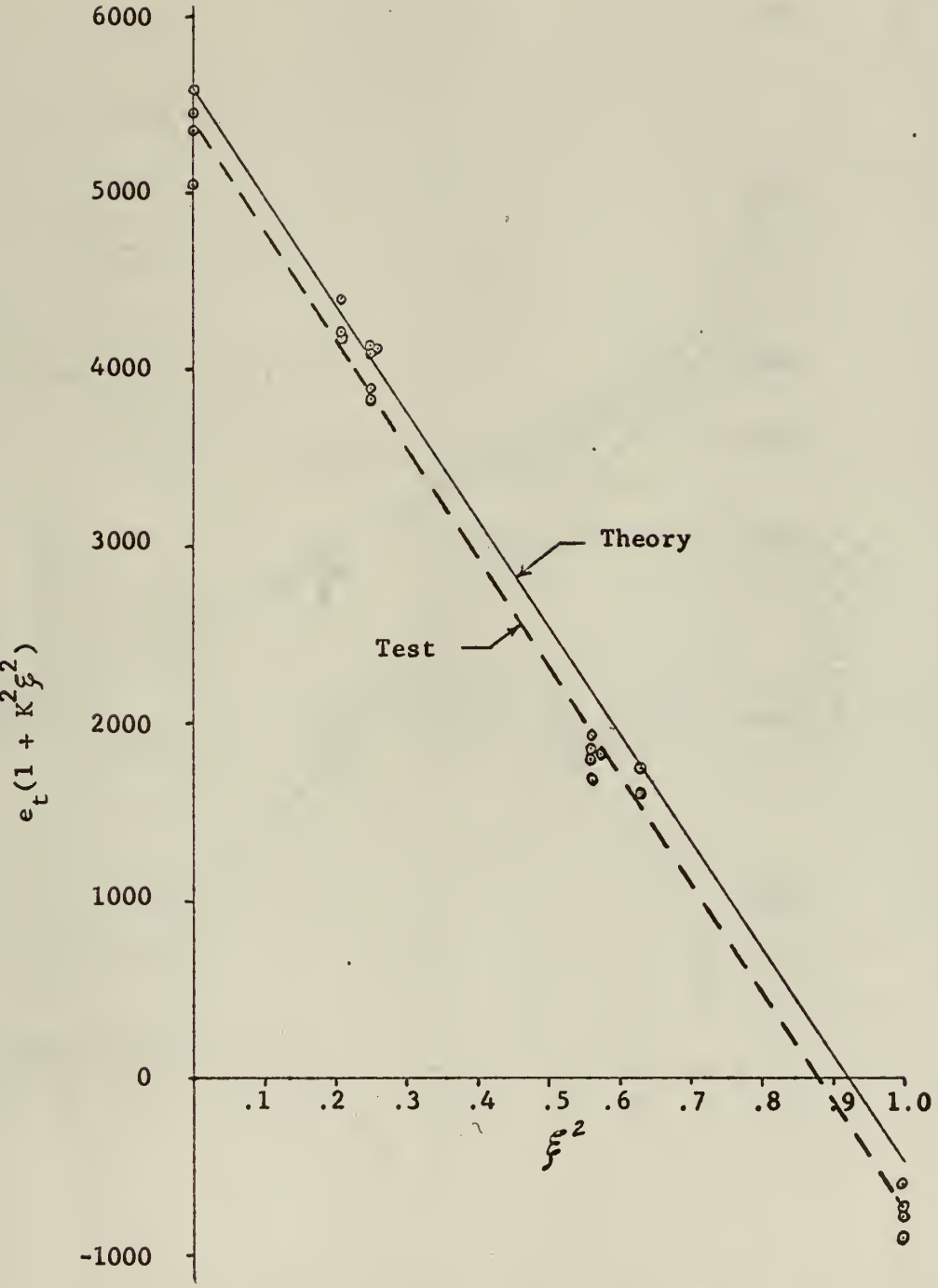

Fig. 19. Strain Distribution Across the Chord, Specimen #1, Test I (P = 10,000 pounds).

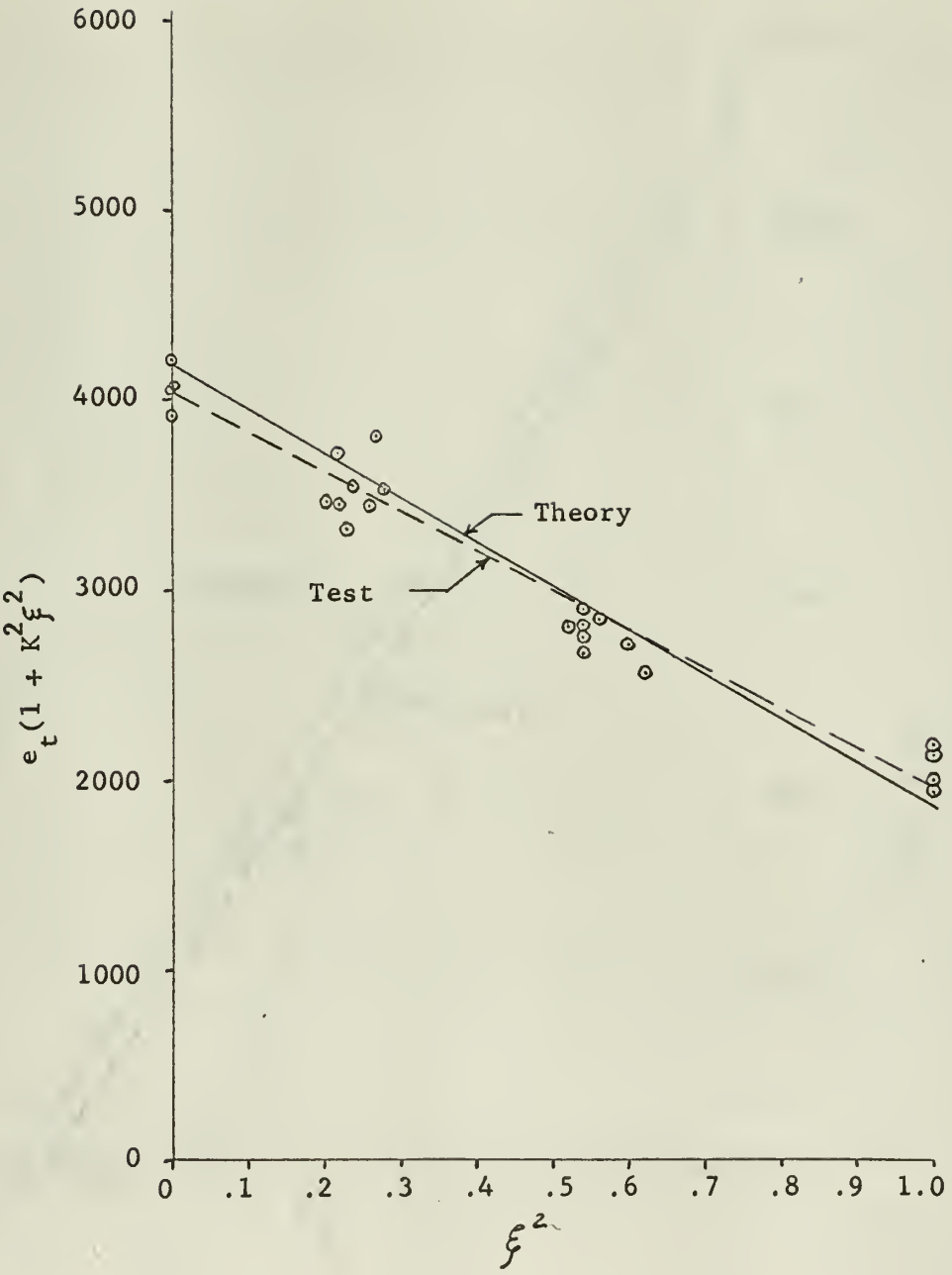

Fig. 20. Strain Distribution Across the Chord, Specimen #2, Test I (P = 10,000 pounds).

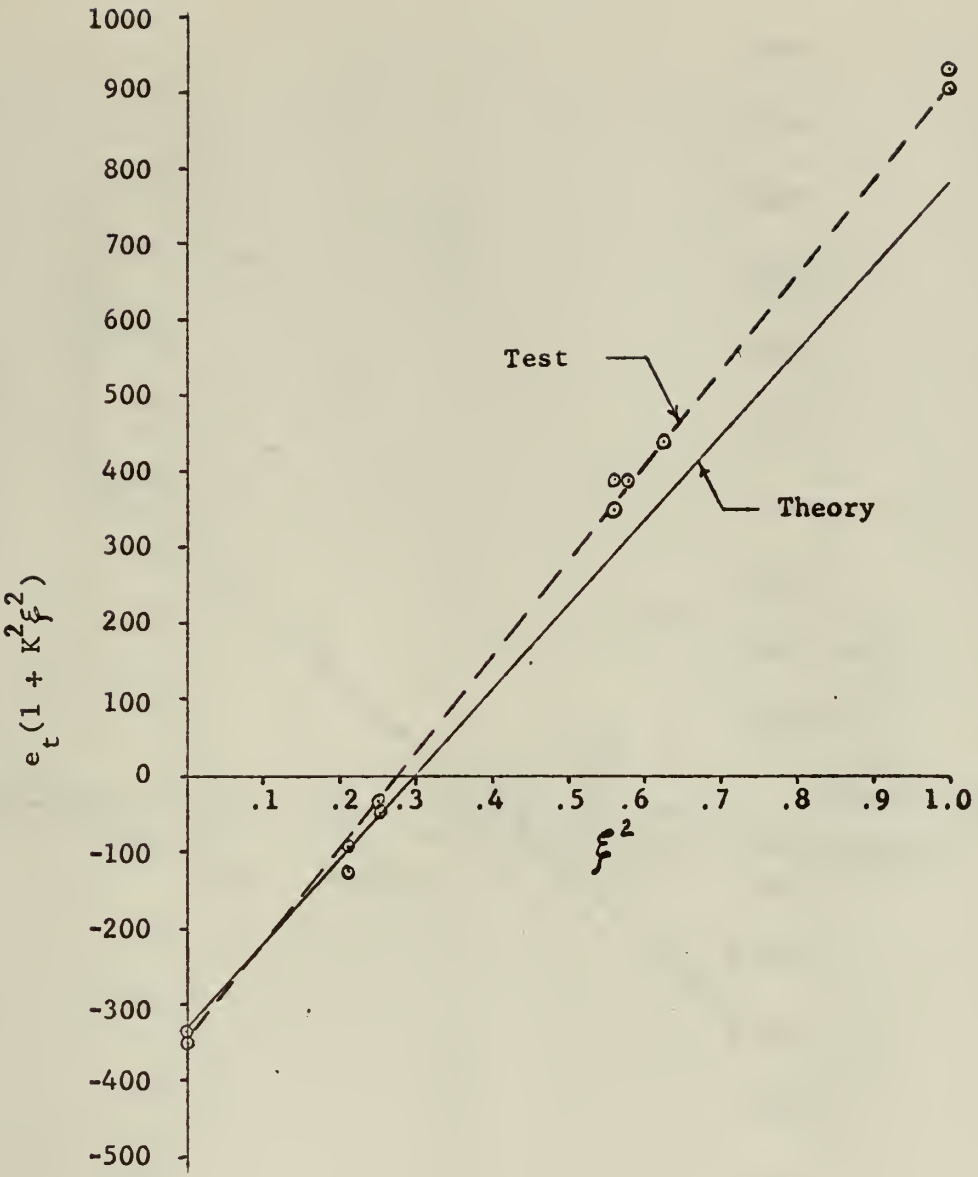

Fig. 21. Strain Distribution Across the Chord, Specimen #1, Test II (T = 120 inch pounds).

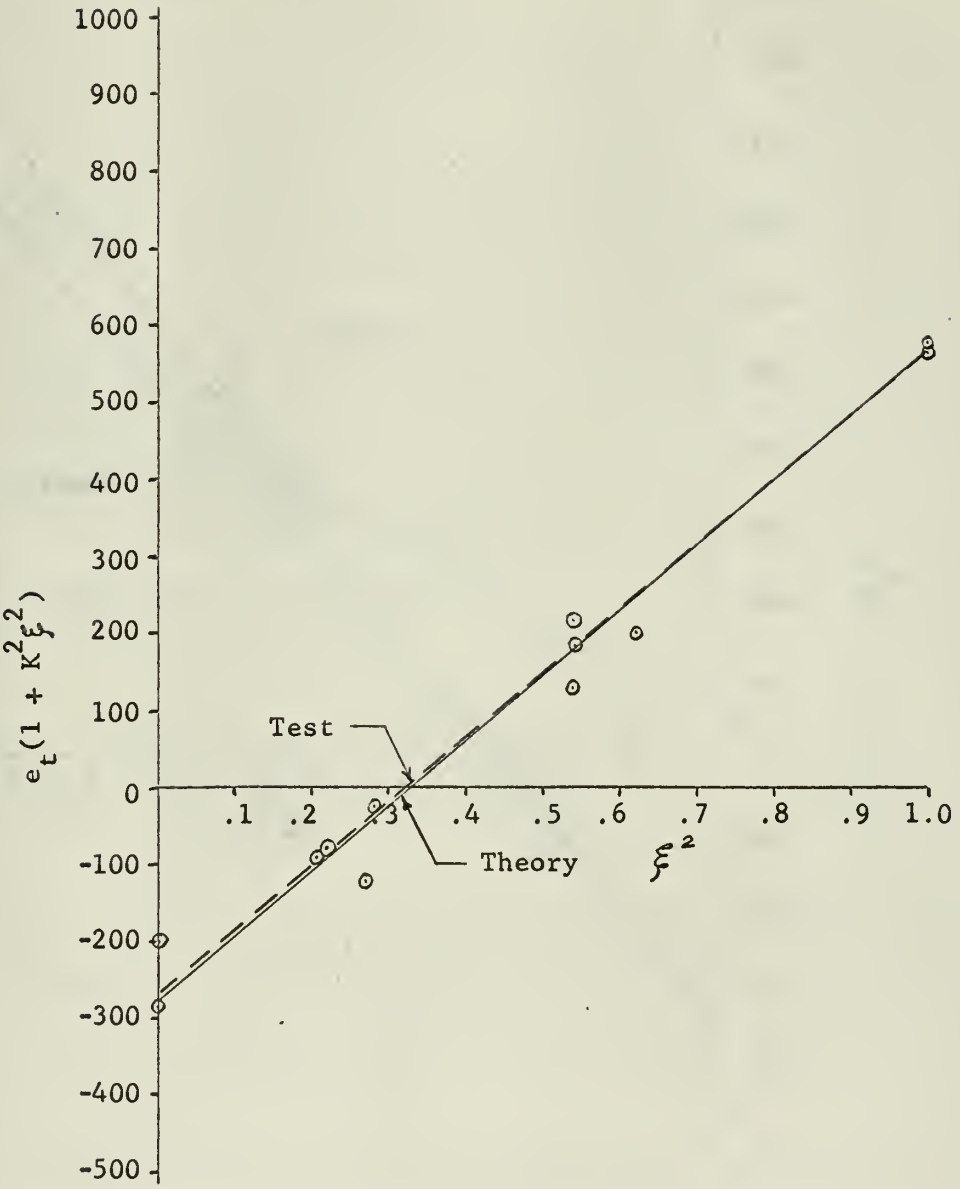

Fig. 22. Strain Distribution Across the Chord, Specimen #2, Test II (T = 129 inch pounds).

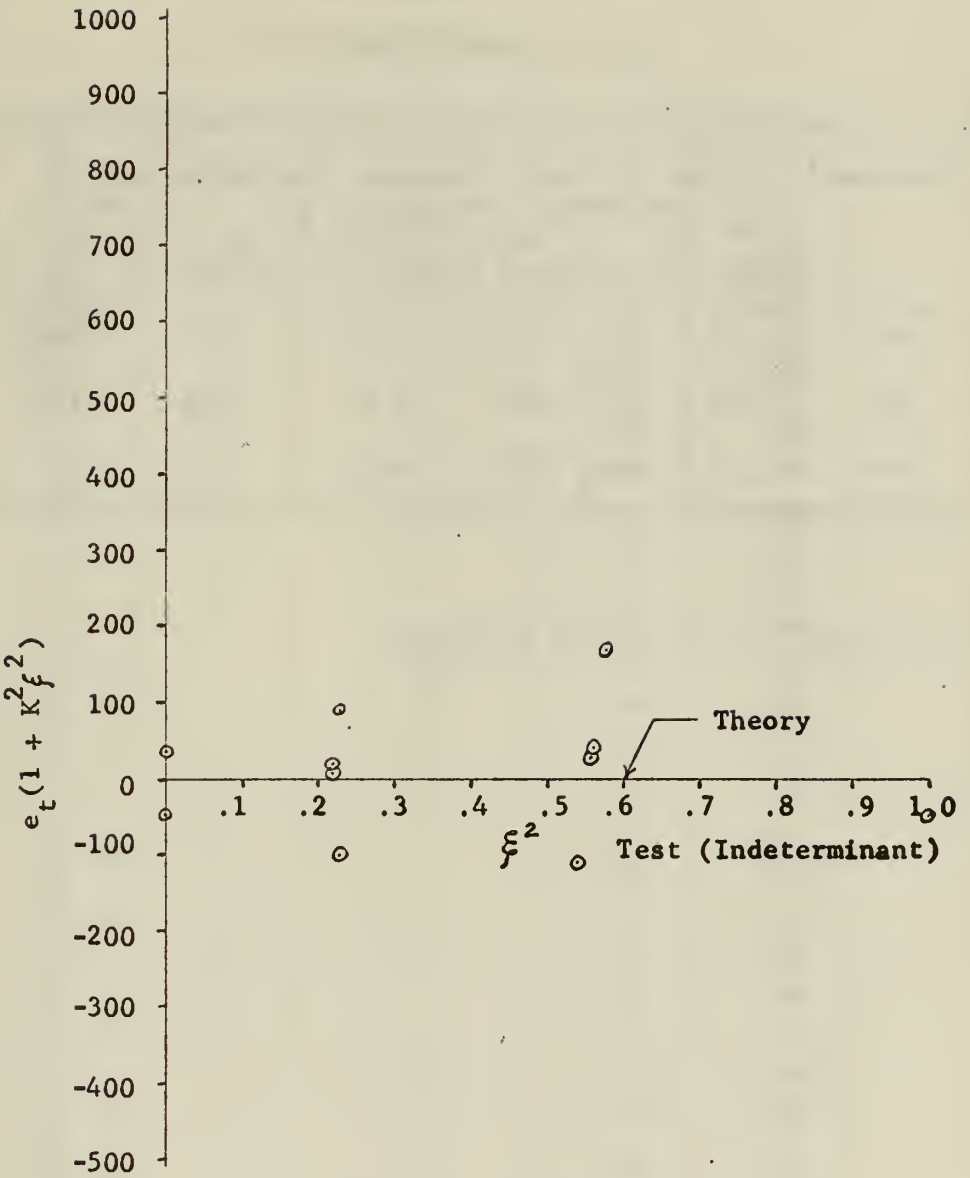

Fig. 23. Strain Distribution Across the Chord, Specimen #3, Test II.

APPENDIX A

TABLE II

TEST SPECIMEN SPECIFICATIONS

Specimen[1]	Cross Section			Blade Length (in.)	dθ/dz (rad/in.)	K	ϕ_{max}
	a (in.)	h (in.)	h_{avg} (in.)				
#1	.75	.200	.182	9.3	.3927	.2945	.2864
#2	.75	.200	.196	9.2	.1963	.1473	.1473
#3	.75	.200	.200	12.7	0	0	0

[1] γ = R/h = 3.125 for all specimens

TABLE III

STRAIN GAGE PLACEMENT

SPECIMEN #1

Gage[1] Number	Gage[2] Type	Gage[3] Factor	℄ Distance	ξ^2
1	A	1.99	0.563	0.563
2	↓	↓	.563	.563
3			0.000	0.000
4			0.000	0.000
5			.594	.626
6			.563	.563
7			.563	.563
8			.563	.563
9			0.000	0.000
10			0.000	0.000
11			.563	.563
12			.594	.626
13			.344	.210
14			.344	.210
19			.375	.250
20			.375	.250
25			.344	.210
26[4]			.375	.250
31			.375	.250
32	↓	↓	.375	.250
37	B	2.10	.750	1.000
38	↓	↓	.750	1.000
39			.750	1.000
40	↓	↓	.750	1.000

[1]Listed so the "back to back" gages appear as a pair.

[2]"A" corresponds to type A-7. "B" corresponds to type FAP 12-12 (S13).

[3]All gage resistances are 120 $\pm$ .5 ohms.

[4]Faulty gage.

TABLE IV

STRAIN GAGE PLACEMENT

SPECIMEN #2

Gage[1] Number	Gage[2] Type	Gage[3] Factor	℄ Distance	ξ^2
1	A	1.99	0.58	0.598
2	A	1.99	.54	.518
3	B	2.09	0.00	0.000
4	B	2.09	0.00	0.000
5	A	1.99	.55	.538
6	B	2.09	.56	.558
7	B	2.09	.38	.257
8	B	2.09	.35	.218
9	A	1.99	.36	.230
10	B	2.09	.37	.243
11	A	1.99	.34	.205
12	B	2.09	.40	.284
13	B	2.09	.39	.270
14	B	2.09	.35	.218
15	A	1.99	.55	.538
16	A	1.99	.59	.619
17	B	2.09	0.00	0.000
18	B	2.09	0.00	0.000
19	A	1.99	.55	.538
20	A	1.99	.55	.538
21	B	2.10	.75	1.000
22	B	2.10	.75	1.000
23	B	2.10	.75	1.000
24	B	2.10	.75	1.000

[1]Listed so the "back to back" gages appear as a pair.

[2]"A" corresponds to type A-7. "B" corresponds to type FAP 12-12 (S13).

[3]All gage resistances are 120 $\pm$ .5 ohms.

TABLE V

STRAIN GAGE PLACEMENT

SPECIMEN #3

Gage[1] Number	Gage Type	Gage[2] Factor	℄ Distance	ξ[2]
3	FAP 12-12	2.09	0.00	0.00
9	↓	↓	0.00	0.00
2			.35	.22
10			.36	.23
4			.36	.23
8			.35	.22
1			.56	.56
11			.55	.54
5			.57	.58
7			.56	.56
6[3]			.75	1.00
12	↓	↓	.75	1.00

[1]Listed so the "back to back" gages appear as a pair.

[2]All gage resistances are 120 ± .5 ohms.

[3]Faulty gage.

TABLE VI

TEST I DATA, SPECIMEN #1

P (pounds)	2000	4000	6000	8000	10000
$P^* \times 10^3$	.66	1.32	1.98	2.64	3.30
ψ (1/16 inch)[1]	10	20	30	40	50
$\chi \times 10^3$	4.4	8.8	13.2	17.6	22.0
Gage Number	Strain (microinches per inch)				
1	350	715	1080	1460	1860
2	325	670	1020	1400	1780
3	1100	2200	3280	4370	5440
4	1075	2150	3220	4280	5340
5	280	580	880	1200	1530
6	350	720	1100	1490	1890
7	325	650	1000	1350	1720
8	325	660	1010	1370	1750
9	1020	2030	3040	4040	5040
10	1120	2230	3350	4460	5570
11	300	600	920	1250	1600
12	310	630	960	1310	1670
13	860	1730	2600	3490	4380
14	830	1650	2480	3320	4160
19	810	1620	2430	3260	4090
20	750	1520	2290	3080	3880
25	820	1640	2490	3350	4210
26[2]					
31	740	1490	2250	3040	3820
32	800	1620	2440	3270	4100
37	-190	-350	-490	-600	-700
38	-150	-280	-390	-480	-540
39	-170	-320	-460	-570	-660
40	-200	-380	-540	-670	-790
$e_o \times 10^3$ avg	1.08	2.15	3.22	4.29	5.35

[1] See eqn. (48).

[2] Faulty gage.

TABLE VII

TEST I DATA, SPECIMEN #2

P (pounds)	2000	4000	6000	8000	10000
$P^* \times 10^3$	0.66	1.32	1.98	2.64	3.30
Ψ (1/16 inch)[1]	6.40	12.8	19.2	25.2	31.2
$\chi \times 10^3$	2.85	5.70	8.54	11.21	13.88
Gage Number	Strain (microinches per inch)				
1	520	1060	1610	2160	2720
2	560	1120	1680	2250	2820
3	810	1620	2440	3245	4060
4	820	1630	2450	3265	4080
5	510	1040	1570	2130	2680
6	535	1080	1650	2240	2840
7	685	1370	2070	2760	3460
8	700	1400	2080	2790	3470
9	650	1310	1980	2660	3345
10	700	1400	2120	2830	3560
11	700	1400	2100	2800	3480
12	700	1400	2120	2830	3550
13	770	1535	2310	3070	3820
14	750	1490	2240	3000	3740
15	550	1110	1680	2250	2830
16	490	1000	1520	2040	2570
17	840	1680	2530	3370	4220
18	770	1560	2350	3140	3930
19	570	1160	1740	2330	2910
20	530	1075	1620	2190	2760
21	400	800	1235	1670	2120
22	350	720	1120	1540	1970
23	340	710	1100	1510	1930
24	385	750	1190	1620	2055
$e_o \times 10^3$ avg	.81	1.62	2.44	3.26	4.07

[1]See eqn. (48).

TABLE VIII

TEST I DATA, SPECIMEN #3

P (pounds)	2000	4000	6000	8000	10000
$P^* \times 10^3$	.66	1.32	1.98	2.64	3.30
φ (1/16 inch)[1]	0	0	0	0	0
$\chi \times 10^3$	0	0	0	0	0
Gage Number	Strain (microinches per inch)				
3	650	1320	1990	2670	3340
9	675	1355	2030	2710	3400
2	650	1310	1975	2650	3320
10	665	1355	2030	2710	3390
4	650	1305	1970	2650	3330
8	660	1330	2000	2680	3360
1	650	1320	2000	2690	3370
11	665	1345	2020	2700	3380
5	645	1295	1955	2630	3310
7	665	1345	2010	2700	3380
6[2]					
12	665	1345	2015	2700	3380
$e_o \times 10^3$ avg	.66	1.34	2.10	2.69	3.37

[1]See eqn. (48).

[2]Faulty gage.

TABLE IX

TEST II DATA, SPECIMEN #1

T (inch pounds)	30	46	85	120	150	180	210
$T^* \times 10^6$	13.1	24.4	37.0	52.2	65.3	78.3	91.4
ψ (1/16 inch)[1]	2.7	4.9	7.3	10.1	12.8	15.1	17.7
$\chi \times 10^3$	1.19	2.17	3.21	4.44	5.63	6.64	7.79
Gage Number	Strain (microinches per inch)						
1	100	181	273	373	463	545	635
2	98	180	267	370	460	540	625
3	-95	-170	-256	-349	-430	-510	-590
4	-88	-158	-242	-332	-410	-485	-565
5	105	198	303	419	520	615	715
6	83	158	240	329	410	485	560
13	-21	-41	-70	-95	-123	-144	-169
14	-33	-62	-86	-123	-154	-183	-212
19	-10	-16	-26	-34	-42	-50	-56
20	-18	-25	-33	-45	-56	-67	-80
37	221	409	620	855	1060	1255	1455
38	214	398	600	825	1020	1210	1400
$e_o \times 10^6_{avg}$	-92	-164	-249	-341	-420	-497	-577

[1] See eqn. (48).

TABLE X

TEST II DATA, SPECIMEN #2

T (inch pounds)	24	49	75	104	129	153	182
$T^* \times 10^6$	10.56	21.56	33.00	45.76	56.76	67.32	80.08
Ψ (1/16 inch)[1]	2.4	5.3	7.8	10.6	13.3	15.3	17.9
$\chi \times 10^3$	1.07	2.36	3.47	4.72	5.92	6.81	7.97
Gage Number	Strain (microinches per inch)						
11	-15	-34	-52	-74	-87	-104	-123
12	-1	-8	-13	-18	-21	-26	-27
13	-25	-48	-70	-97	-121	-142	-167
14	-15	-28	-45	-65	-76	-91	-104
15	41	76	113	152	186	216	247
16	39	82	121	163	202	237	272
17	-58	-112	-168	-231	-283	-332	-387
18	-41	-79	-118	-161	-198	-230	-268
19	28	54	81	108	132	153	176
20	41	89	127	179	220	257	300
23	115	229	343	468	575	670	778
24	112	223	333	457	559	652	755
$e_o \times 10^6$ avg	-50	-96	-143	-196	-240	-281	-328

[1]See eqn. (48).

TABLE XI

TEST II DATA, SPECIMEN #3

T (inch pounds)	16	33	49	68	86	107	126
T* x 10^6	7.0	14.5	21.6	29.9	37.8	47.1	55.4
ψ (1/16 inch)[1]	2.4	5.2	7.5	10.4	13.4	16.3	19.1
χ x 10^3	.77	1.67	2.42	3.35	4.31	5.25	6.15
Gage Number	Strain (microinches per inch)						
3	-2	-6	-15	-21	-25	-30	-36
9	5	10	16	23	29	36	45
2	-1	-4	-7	-15	-15	-20	-24
10	12	27	41	57	67	84	99
4	-12	-23	-38	-50	-64	-79	-93
8	-1	-2	-6	-8	-12	-11	-12
1	-4	-10	-14	-23	-31	-38	-44
11	17	30	48	63	77	93	110
5	-21	-40	-68	-92	-117	-147	-171
7	-5	-10	-14	-18	-21	-26	-31
6[2]							
12	12	18	27	33	38	43	48
e_o x 10^6 avg	1.5	2.0	0.5	1.0	2.0	3.0	4.0

[1]See eqn. (48).

[2]Faulty gage.

APPENDIX B

Calculation of Young's Modulus, E.

From Fig. 13:

$P = 10{,}000$ pounds

$e_{t_{avg}} = 336 \times 10^{-6}$ inches/inch

$$E = \frac{P}{Ae_t} = \frac{P}{2ahe_t} = \frac{10000}{2(.75)(.2)(.000336)} = 10.1 \times 10^6 \text{ psi}$$

Calculation of α Coefficients.

The calculation of the first three α coefficients involves the solution of the appropriate integrals in eqns. (29) and (30). These can be broken down into basic integrals of the form

$$\int_0^1 \frac{\xi^n}{(1+K^2\xi^2)^2}\, d\xi$$

where n = 0, 2, and 4. These integrals will be referred to as I_1, I_2, and I_3, respectively.

$$I_1 = \int_0^1 \frac{1}{(1+K^2\xi^2)^2}\, d\xi = \frac{1}{2(1+K^2)} + \frac{1}{2K}\tan^{-1}K$$

but $\frac{1}{1+K^2} = 1 - K^2 + K^4 - K^6 + \cdots\cdots$

and $\tan^{-1} K = K - \frac{1}{3}K^3 + \frac{1}{5}K^5 + \cdots\cdots$

Substituting,

$$I_1 = \frac{1}{2}\left[(1-\kappa^2+\kappa^4+\cdots)+(1-\tfrac{1}{3}\kappa^2+\tfrac{1}{5}\kappa^4+\cdots)\right]$$

$$I_1 = 1 - \frac{2}{3}\kappa^2 + \frac{3}{5}\kappa^4 + \cdots$$

$$I_2 = \int_0^1 \frac{\xi^2}{(1+\kappa^2\xi^2)^2}\,d\xi = \frac{-1}{2\kappa^2(1+\kappa^2)} + \frac{1}{2\kappa^3}\tan^{-1}\kappa$$

$$I_2 = \frac{1}{2}\left[\left(\frac{-1}{\kappa^2}+1-\kappa^2+\kappa^4+\cdots\right)+\left(\frac{1}{\kappa^2}-\frac{1}{3}+\frac{1}{5}\kappa^2-\frac{1}{7}\kappa^4+\cdots\right)\right]$$

$$I_2 = \frac{1}{3} - \frac{2}{5}\kappa^2 + \frac{3}{7}\kappa^4 + \cdots$$

$$I_3 = \int_0^1 \frac{\xi^4}{(1+\kappa^2\xi^2)^2}\,d\xi = \frac{1}{\kappa^2(1+\kappa^2)} - \frac{3}{\kappa^2} I_2$$

$$I_3 = \frac{1}{\kappa^2}\left[(1-\kappa^2+\kappa^4-\kappa^6+\cdots)-(1-\tfrac{6}{5}\kappa^2+\tfrac{9}{7}\kappa^4-\tfrac{12}{9}\kappa^6+\cdots)\right]$$

$$I_3 = \frac{1}{5} - \frac{2}{7}\kappa^2 + \frac{3}{9}\kappa^4 + \cdots$$

From eqns. (29) and (30),

$$\alpha_{11} = I_1 - \tau\kappa^2 I_2 = (1-\tfrac{2}{3}\kappa^2+\tfrac{3}{5}\kappa^4+\cdots)-\tau(\tfrac{1}{3}\kappa^2-\tfrac{2}{5}\kappa^4+\cdots)$$

$$\alpha_{11} = 1 - \frac{1}{3}(2+\tau)\kappa^2 + \frac{1}{5}(3+2\tau)\kappa^4 + \cdots$$

$$\alpha_{12} = \alpha_{21} = \kappa I_2 - \tau\kappa^3 I_3$$

$$\alpha_{12} = (\tfrac{1}{3}\kappa - \tfrac{2}{5}\kappa^3 + \tfrac{3}{7}\kappa^5+\cdots) - \tau(\tfrac{1}{5}\kappa^3 - \tfrac{2}{7}\kappa^5+\cdots)$$

$$\alpha_{12} = \frac{1}{3}K - \frac{1}{5}(2+\tau)K^3 + \frac{1}{7}(3+2\tau)K^5 + \cdots$$

From eqn. (47),

$$\alpha_{22} = \frac{G h_{avg}^2 (.667a - .21 h_{avg})\left[1 + \frac{2}{15}(1+\mu)\left(\phi_{max}\frac{2a}{h_{avg}}\right)^2\right]}{2a^3E} + \frac{\alpha_{12}^2}{\alpha_{11}} \qquad (47)$$

Substituting into the above three expressions for α_{11}, α_{12}, and α_{22}, there is

$$\alpha_{11})_1 = 1 - .148 + .014 = .866$$

$$\alpha_{11})_2 = 1 - .037 = .963$$

$$\alpha_{11})_3 = 1$$

$$\alpha_{12})_1 = .0982 - .0262 + .0029 = .0749$$

$$\alpha_{12})_2 = .0491 - .0033 = .046$$

$$\alpha_{12})_3 = 0$$

$$\alpha_{22})_1 = \frac{3.9 \times 10^6 (.182)^2}{2(.75)^3 10.1 \times 10^6}\left\{[.667(.75) - .21(.182)]\left[1 + \frac{2}{15}(1+.33)\left(.2864\,\frac{1.5}{.182}\right)^2\right]\right\} + \frac{(.0749)^2}{.866}$$

$$\alpha_{22})_1 = .01516(.5 - .0382)(1 + .988) + .0065$$

$$\alpha_{22})_1 = .0139 + .0065 = .0204$$

$$\alpha_{22})_2 = .0176(.5 - .0412)(1 + .222) + .0022$$

$$\alpha_{22})_2 = .00986 + .0022 = .0121$$

$$\alpha_{22})_3 = .0183(.5 - .042)\ (1) + 0 = .00838$$

Calculation of β coefficients.

The expressions for β coefficients in terms of α coefficients are to be found in eqns. (33) and (34). Let

$$D = \alpha_{11}\alpha_{22} - \alpha_{12}^2$$

$$\beta_{11} = \frac{\alpha_{22}}{D}$$

$$\beta_{12} = \frac{-\alpha_{12}}{D}$$

$$\beta_{22} = \frac{\alpha_{11}}{D}$$

$$D_1 = (.866)(.0204) - (.0749)^2 = .0121$$

$$\beta_{11})_1 = (.0204)/(.0121) = 1.69$$

$\beta_{12})_1 = (-.0749)/(.0121) = -6.21$

$\beta_{22})_1 = (.866)/(.0121) = 71.8$

$D_2 = (.963)(.0121) - (.046)^2 = .00954$

$\beta_{11})_2 = (.0121)/(.00954) = 1.27$

$\beta_{12})_2 = (-.046)/(.00954) = -4.82$

$\beta_{22})_2 = (.963)/(.00954) = 101$

$D_3 = (1)\ (.00838) = .00838$

$\beta_{11})_3 = (.00838)/(.00838) = 1.0$

$\beta_{12})_3 = 0$

$\beta_{22})_3 = (.963)/(.00838) = 119.3$

Calculation of theoretical strain distribution.

The theoretical strain distribution across the chord is given by eqn. (25).

$$e_t\ (1 + K^2\xi^2) = e_o + \chi K \xi^2 \qquad (25)$$

a) Test I: P = 10,000 pounds, T = 0

From eqns. (35) and (36)

$$e_o = \beta_{11} P^*$$

$$\chi = \beta_{21} P^*$$

Specimen #1:

$$e_o = 1.69(3300 \times 10^{-6}) = 5577 \times 10^{-6}$$

$$\chi = -6.21(3300 \times 10^{-6}) = -20500 \times 10^{-6}$$

$$e_t(1 + K^2\xi^2) = 5577 \times 10^{-6} - 20500 \times 10^{-6}(.2945)\xi^2$$

$$e_t(1 + K^2\xi^2) = 5577 \times 10^{-6} - 6035 \times 10^{-6}\xi^2$$

Specimen #2:

$$e_o = 1.27(3300 \times 10^{-6}) = 4191 \times 10^{-6}$$

$$\chi = -4.82(3300 \times 10^{-6}) = -15,906 \times 10^{-6}$$

$$e_t(1 + K^2\xi^2) = 4191 \times 10^{-6} - 15,906 \times 10^{-6}(.1473)\xi^2$$

$$e_t(1 + K^2\xi^2) = 4191 \times 10^{-6} - 2343 \times 10^{-6}\xi^2$$

Specimen #3:

$$e_o = 1.0(3300 \times 10^{-6}) = 3300 \times 10^{-6}$$

$$\chi = 0$$

$$e_t(1 + K^2\xi^2) = 3300 \times 10^{-6}$$

b) Test II: T ≅ 125 inch pounds, P = 0

From eqns. (35) and (36)

$$e_o = \beta_{12} T^*$$

$$\chi = \beta_{22} T^*$$

Specimen #1:

$$e_o = -6.21(52.2 \times 10^{-6}) = -324 \times 10^{-6}$$

$$\chi = 71.8(52.2 \times 10^{-6}) = 3748 \times 10^{-6}$$

$$e_t(1 + K^2\xi^2) = -324 \times 10^{-6} + 3748 \times 10^{-6}(.2945)\xi^2$$

$$e_t(1 + K^2\xi^2) = -324 \times 10^{-6} + 1103 \times 10^{-6}\xi^2$$

Specimen #2:

$$e_o = -4.82(56.76 \times 10^{-6}) = -273 \times 10^{-6}$$

$$\chi = 101(56.76 \times 10^{-6}) = 5733 \times 10^{-6}$$

$$e_t(1 + K^2\xi^2) = -273 \times 10^{-6} + 5733 \times 10^{-6}(.1473)\xi^2$$

$$e_t(1 + K^2\xi^2) = -273 \times 10^{-6} + 844 \times 10^{-6}\xi^2$$

Specimen #3:

$$e_o = 0$$

$$\chi = 119.3(55.4 \times 10^{-6}) = 6610 \times 10^{-6}$$

$$e_t(1 + K^2\xi^2) = 0(6610 \times 10^{-6})\xi^2 = 0$$

INITIAL DISTRIBUTION LIST

		No. Copies
1.	Defense Documentation Center Cameron Station Alexandria, Virginia 22314	20
2.	Library U. S. Naval Postgraduate School, Monterey, California	2
3.	Commander, Naval Air Systems Command Department of the Navy Washington, D.C. 20360	1
4.	Professor T. H. Gawain Department of Aeronautics U. S. Naval Postgraduate School Monterey, California	1
5.	Chairman Department of Aeronautics U. S. Naval Postgraduate School Monterey, California	1
6.	LCDR L. M. Hogan, USN 27 Revere Road Monterey, California	1

UNCLASSIFIED

Security Classification

DOCUMENT CONTROL DATA - R&D

(Security classification of title, body of abstract and indexing annotation must be entered when the overall report is classified)

1. ORIGINATING ACTIVITY (Corporate author)	2a. REPORT SECURITY CLASSIFICATION
U. S. Naval Postgraduate School Monterey, California	UNCLASSIFIED
	2b. GROUP

3. REPORT TITLE

STRESS DISTRIBUTION AND DEFORMATION IN A TWISTED BLADE UNDER COMBINED TENSION AND TORSION

4. DESCRIPTIVE NOTES (Type of report and inclusive dates)

Thesis for Master of Science in Aeronautical Engineering

5. AUTHOR(S) (Last name, first name, initial)

Hogan, Lawrence M., LCDR, USN

6. REPORT DATE	7a. TOTAL NO. OF PAGES	7b. NO. OF REFS
May 1966	80	6

8a. CONTRACT OR GRANT NO.	9a. ORIGINATOR'S REPORT NUMBER(S)
b. PROJECT NO.	
c.	9b. OTHER REPORT NO(S) (Any other numbers that may be assigned this report)
d.	

10. AVAILABILITY/LIMITATION NOTICES

[redacted] Memorandum 12/16/69

This document has been approved for public release and sale; its distribution is unlimited.

11. SUPPLEMENTARY NOTES	12. SPONSORING MILITARY ACTIVITY
	Commander, Naval Air Systems Command Navy Department, Washington, D.C.

13. ABSTRACT

This report is a theoretical and experimental investigation of the stress distribution and deformation of twisted blades under combined tension and torsion. Theoretical expressions were developed to relate the deformation of a twisted "blade" of rectangular cross section and constant rate of twist to an applied load and moment. These expressions were found to be linear for the rates of twist investigated and depended only on the blade material and geometry. The theoretical strain distribution was found to be essentially parabolic across the chord, with the shape determined by the initial twist rate and the angular deformation.

The experimental investigation was conducted with three specimens of constant cross sectional aspect ratio but different rates of twist. Correlation with theory was found to be excellent for the chordwise distribution of strain and generally good for the linear relationships linking the deformation with the applied loads. Recommendations were made for areas of further investigation.

DD FORM 1 JAN 64 1473

UNCLASSIFIED

Security Classification

14. KEY WORDS	LINK A		LINK B		LINK C	
	ROLE	WT	ROLE	WT	ROLE	WT
Stress Distribution Deformation Torsion Twisted Blade Twisted Bar Tension						

INSTRUCTIONS

1. ORIGINATING ACTIVITY: Enter the name and address of the contractor, subcontractor, grantee, Department of Defense activity or other organization *(corporate author)* issuing the report.

2a. REPORT SECURITY CLASSIFICATION: Enter the overall security classification of the report. Indicate whether "Restricted Data" is included. Marking is to be in accordance with appropriate security regulations.

2b. GROUP: Automatic downgrading is specified in DoD Directive 5200.10 and Armed Forces Industrial Manual. Enter the group number. Also, when applicable, show that optional markings have been used for Group 3 and Group 4 as authorized.

3. REPORT TITLE: Enter the complete report title in all capital letters. Titles in all cases should be unclassified. If a meaningful title cannot be selected without classification, show title classification in all capitals in parenthesis immediately following the title.

4. DESCRIPTIVE NOTES: If appropriate, enter the type of report, e.g., interim, progress, summary, annual, or final. Give the inclusive dates when a specific reporting period is covered.

5. AUTHOR(S): Enter the name(s) of author(s) as shown on or in the report. Enter last name, first name, middle initial. If military, show rank and branch of service. The name of the principal author is an absolute minimum requirement.

6. REPORT DATE: Enter the date of the report as day, month, year; or month, year. If more than one date appears on the report, use date of publication.

7a. TOTAL NUMBER OF PAGES: The total page count should follow normal pagination procedures, i.e., enter the number of pages containing information.

7b. NUMBER OF REFERENCES: Enter the total number of references cited in the report.

8a. CONTRACT OR GRANT NUMBER: If appropriate, enter the applicable number of the contract or grant under which the report was written.

8b, 8c, & 8d. PROJECT NUMBER: Enter the appropriate military department identification, such as project number, subproject number, system numbers, task number, etc.

9a. ORIGINATOR'S REPORT NUMBER(S): Enter the official report number by which the document will be identified and controlled by the originating activity. This number must be unique to this report.

9b. OTHER REPORT NUMBER(S): If the report has been assigned any other report numbers *(either by the originator or by the sponsor)*, also enter this number(s).

10. AVAILABILITY/LIMITATION NOTICES: Enter any limitations on further dissemination of the report, other than those imposed by security classification, using standard statements such as:

(1) "Qualified requesters may obtain copies of this report from DDC."

(2) "Foreign announcement and dissemination of this report by DDC is not authorized."

(3) "U. S. Government agencies may obtain copies of this report directly from DDC. Other qualified DDC users shall request through _____."

(4) "U. S. military agencies may obtain copies of this report directly from DDC. Other qualified users shall request through _____."

(5) "All distribution of this report is controlled. Qualified DDC users shall request through _____."

If the report has been furnished to the Office of Technical Services, Department of Commerce, for sale to the public, indicate this fact and enter the price, if known.

11. SUPPLEMENTARY NOTES: Use for additional explanatory notes.

12. SPONSORING MILITARY ACTIVITY: Enter the name of the departmental project office or laboratory sponsoring *(paying for)* the research and development. Include address.

13. ABSTRACT: Enter an abstract giving a brief and factual summary of the document indicative of the report, even though it may also appear elsewhere in the body of the technical report. If additional space is required, a continuation sheet shall be attached.

It is highly desirable that the abstract of classified reports be unclassified. Each paragraph of the abstract shall end with an indication of the military security classification of the information in the paragraph, represented as *(TS)*, *(S)*, *(C)*, or *(U)*.

There is no limitation on the length of the abstract. However, the suggested length is from 150 to 225 words.

14. KEY WORDS: Key words are technically meaningful terms or short phrases that characterize a report and may be used as index entries for cataloging the report. Key words must be selected so that no security classification is required. Identifiers, such as equipment model designation, trade name, military project code name, geographic location, may be used as key words but will be followed by an indication of technical context. The assignment of links, roles, and weights is optional.

DD FORM 1 JAN 64 1473 (BACK)